OBSERVATIONS OF THE NIAGARA RIVER THERMAL FRONT

A.K. Masse and C.R. Murthy

NWRI Contribution No. 89-35

Lakes Research Branch
National Water Research Institute
Canada Centre for Inland Waters
Burlington, Ontario L7R 4A6
Canada

July 1989

ABSTRACT

The mixing between the Niagara River and Lake Ontario has a critical impact on the coastal Lake Ontario environment. The Niagara River provides the bulk of materials that flow into Lake Ontario, including toxic contaminants. This study shows that the thermal fronts created by the Niagara River play a crucial role in the exchange of water between river and lake. The Niagara River discharge into Lake Ontario forms a plume bounded by strong horizontal gradients or fronts. The variable nature of these fronts are examined using temperature and velocity data from a 1982 study of the Niagara River plume by Murthy et al. (1984). Results show that the earth's rotation is important to the plume and frontal dynamics. The action of Coriolis force concentrates the plume along the coast to the right, when viewed facing offshore. Exchange between the plume and the lake is enhanced by upwelling favorable winds and inhibited by downwelling favorable winds.

RÉSUMÉ

Le mélange entre la rivière Niagara et le lac Ontario a un impact profond sur l'environnement riverain du lac. La Niagara apporte le plus gros des matières qui entrent dans le lac, dont des contaminants toxiques. Cette étude montre que les fronts thermiques créés par la Niagara jouent un rôle crucial dans l'échange d'eau entre la rivière et le lac. L'écoulement de la Niagara forme un panache délimité par de forts gradients horizontaux ou fronts. La nature de ces fronts est étudiée à l'aide des données de température et de vitesse d'une étude de 1982 sur le panache de la Niagara par Murthy et al. (1984). Les résultats montrent que la rotation de la Terre est importante dans la dynamique du panache et des fronts. Les forces de Coriolis concentrent le panache le long de la rive à droite, en regardant face au lac. L'échange entre le panache et le lac est accru par les vents ascendants favorables et affaibli par les vents descendants défavorables.

MANAGEMENT PERSPECTIVE

The mixing between the Niagara River and Lake Ontario has a critical impact on the Lake Ontario environment. The Niagara River provides the bulk of materials that flow into Lake Ontario, including toxic contaminants. This study shows that the thermal fronts created by the Niagara River play a crucial role in the exchange of water between river and lake. The Niagara River discharge forms a plume bounded by strong horizontal gradients or fronts. The nature of these fronts are examined using temperature and velocity data from a 1982 study of the Niagara River plume by Murthy et al. (1984). Results show that the earth's rotation is important to the plume and frontal dynamics. The action of the Coriolis force concentrates the plume along the coast to the right, when viewed facing offshore. Exchange between the plume and the lake is enhanced by upwelling favorable winds and inhibited by downwelling favorable winds. The role of the thermal front in the exchange of the Niagara River water with Lake Ontario is discussed. The report provides a basis for the integration of the transport and pathways of toxic contaminants in the Niagara River - Lake Ontario - St. Lawrence River systems.

PERSPECTIVE-GESTION

Le mélange entre la rivière Niagara et le lac Ontario a un impact profond sur l'environnement riverain du lac. La Niagara apporte le plus gros des matières qui entrent dans le lac, dont des contaminants toxiques. Cette étude montre que les fronts thermiques créés par la Niagara jouent un rôle crucial dans l'échange d'eau entre la rivière et le lac. L'écoulement de la Niagara forme un panache délimité par de forts gradients horizontaux ou fronts. La nature de ces fronts est étudiée à l'aide des données de température et de vitesse d'une étude de 1982 sur le panache de la Niagara par Murthy et al. (1984). Les résultats montrent que la rotation de la Terre est importante dans la dynamique du panache et des fronts. Les forces de Coriolis concentrent le panache le long de la rive à droite, en regardant face au lac. L'échange entre le panache et le lac est accru par les vents ascendants favorables et affaibli par les vents descendants défavorables. On envisage le rôle du front thermique dans l'échange de l'eau de la Niagara avec le lac Ontario. Ce

rapport jette les bases d'une intégration du transport et du cheminement des contaminants toxiques dans le système Niagara - lac Ontario - Saint-Laurent.

Acknowledgements

One of us (AKM) was supported through a contract (No. KW405-8-2558/01-SE) by Lakes Research Branch of National Water Research Institute.

Ken Miners and William Schertzer were a great help in locating and interpreting the archived data and programs. Many thanks to both. We thank Mr. L. Benner for carefully redigitizing the data. We also thank Ms. J. Hodson for her assistance with the GPCP contouring package.

LIST OF FIGURES

Figure 3.4. (a) Surface density (σ_t) contours on April 15, 1982 compiled from the first profile taken at each station. (b) Same as (a) but the second profile when taken is used.

Figure 3.5. Surface density (σ_t) contours on (a) May 27, 1982 and (b) May 28, 1982. The contour interval is 0.02 σ_t.

Figure 3.6. (a) Density contours (σ_t) from temperature profiles along alongshore transect 4, located 1.5 kilometers offshore, on May 27, 1982. (b) Density contours (σ_t) from temperature profiles along offshore transect 11 on May 27, 1982. Station 198 is at the river mouth. The contour interval is 0.02 σ_t.

Figure 3.7. Surface density (σ_t) contours on (a) June 21, 1982; (b) June 22, 1982; (c) June 23, 1982; (d) June 24, 1982; and (e) June 25, 1982. The contour interval is 0.05 σ_t.

Figure 3.8. Density contours (σ_t) from temperature profiles along offshore transect 11 on (a) June 22, 1982; (b) June 23, 1982; (c) June 24, 1982; and (d) June 25, 1982. Station 198 is at the river mouth. The contour interval is 0.05 σ_t.

Figure 3.9. Density contours (σ_t) from temperature profiles along alongshore transect 11, located 5 kilometers offshore, on (a) June 24, 1982 and (b) June 25, 1982. The contour interval is 0.05 σ_t.

Figure 3.10. Surface density (σ_t) contours on (a) August 11, 1982 and (b) August 12, 1982. The contour interval is 0.05 σ_t.

Figure 3.11. Density contours (σ_t) from temperature profiles along offshore transect 11 on (a) August 11, 1982 and (b) August 12, 1982. Station 198 is at the river mouth. The contour interval is 0.05 σ_t.

Figure 3.12. Density contours (σ_t) from temperature profiles along (a) alongshore transect 8, located 3.5 kilometers offshore, and (b) alongshore transect 16, located 7.5 kilometers offshore, on August 12, 1982. The contour interval is 0.05 σ_t.

Figure 3.13. Surface density (σ_t) contours on (a) October 5, 1982, (b) October 6, 1982, and (c) October 7, 1982. The contour interval is 0.05 σ_t.

Figure 3.14. Density contours (σ_t) from temperature profiles along (a) alongshore transect 8, located 4.5 kilometers offshore, (b) alongshore transect 14, located 6.5 kilometers offshore, and (c) alongshore transect 20, located 9.5 kilometers offshore, on October 5, 1982. The contour interval is 0.05 σ_t.

Figure 3.15. Density contours (σ_t) from temperature profiles along (a) offshore transect 3, (b) offshore transect 11, station 198 marks the river mouth, and (c) offshore transect 15, on October 5, 1982. The contour interval is 0.05 σ_t.

Figure 3.16. On the left is the surface density (σ_t) contours on November 8, 1982. The contour interval is 0.02 σ_t. On the right are the current vectors estimated from the Lagrangian records of the drogues released at the river mouth on the same day.

Figure 3.17. Same as figure 3.16, except for November 9, 1982.

Figure 3.18. Same as figure 3.16, except for November 10, 1982.

Figure 3.19. Density contours (σ_t) from temperature profiles along offshore transect 11. Station 198 marks the river mouth. The contour interval is 0.02 σ_t.

Figure 4.1. The buoyancy ($B=g'Q$) input by the Niagara River into Lake Ontario during the six experiments. The dates of the experiments are placed along the horizontal axis by experiment and are not to scale.

Figure 4.2. The internal Rossby radius of deformation (R_i) in kilometers of the Niagara River plume over ambient lake water. The dates of the experiments are placed along the horizontal axis by experiment and are not to scale.

Figure 4.3. Diagram of a front between a buoyant spreading layer and denser ambient water. The arrows show fluid motions relative to the movement of the front, from Federov (1986).

Figure 4.4. Diagram of the isotherms in a coastal front due to the differrences in tidal mixing due to a sloping bottom as described by Simpson and Hunter (1974), from Federov (1986).

Figure 4.5. Plume map from the results of Garvine's (1987) estuary plume model where the estuary is perpendicular to the coast. The dashed lines are streamlines of the buoyant plume and the solid lines are the fronts. To the left of the mouth U_a denotes the uniform alongshore current. The x and y axes are scaled by the estuary mouth width.

TABLE OF CONTENTS

1. Introduction

Fronts are regions of intensified horizontal gradients commonly found in shelf seas, estuaries and sometimes in fresh water environments. Frontal zones are regions of strong horizontal convergence, capable of concentrating various pollutants and toxic substances of anthropogenic origin at the water's surface. It follows that fronts play an important role in problems of waste water discharge. In the ocean, fronts are regions of high productivity and, thus, are important to commercial and recreational fishing interests. A similar link between biological production and fronts has not been documented in the fresh water environment and, in general, there has been little research on fresh water fronts.

While the above definition of fronts is general enough to cover most horizontal fluid boundaries, the discussion of fronts in this report is limited to strong horizontal density gradients which outcrop at the free surface. Surface fronts occur over many scales. There are large oceanic fronts of several thousand kilometers, upwelling fronts on the order of tens to hundreds of kilometers and smaller fronts of only a few kilometers associated with the outflow of buoyant water into heavier coastal water.

These smaller scale fronts have been observed on the edges of river and estuary outflow plumes in coastal ocean waters.

Observations of such plumes and their frontal features have been documented for the Connecticut River (Garvine 1974a; Garvine and Monk 1974), the Amazon (Ryther et al. 1967), the Mississippi (Wright and Coleman 1971), the Fraser River (Cordes et al. 1980), the Great Whale River which empties onto Hudson Bay (Ingram 1981), and the outflow of the Chesapeake Bay estuary (Boicourt 1973). In fresh water, fronts often form at the boundary between the outflow of warmer, lighter water into the colder, heavier coastal water of lakes or reservoirs. For example, Scarspace and Green (1973) observed temperature/density fronts bounding the heated water outflow of a power plant into the colder waters of Lake Michigan.

In their work on the Connecticut River plume Garvine and Monk (1974) found strong convergent velocities at the plumes front with velocity shears in excess of 80 cm/s. Throughout their many observations of the front, debris, logs, and chunks of ice were found trapped in the frontal zone. An important conclusion of their work is that most of the mixing between the plume and the coastal water occurs at the front. As the buoyant plume spreads out over the coastal water the heavier fluid is entrained into the plume from below the surface front at the leading edge of the plume.

Garvine and Monk (1974) found the Connecticut River plume front has a time scale of only a few hours. The Connecticut River front and other fronts bounding buoyant plumes in coastal

waters are predominantly dissipated by tidal energy. O'Donnell (1976) has shown with a time dependent numerical model that the tidal currents are important to the formation and strength of fronts, which are related to the mixing intensity at the front.

In this study the outflow of the Niagara River into Lake Ontario is examined with particular attention to the fronts bounding the outflow plume. The Niagara River flows from Lake Erie to Lake Ontario passing through densely populated industrial areas on the Canadian and U.S. borders. This region is known for its toxic 'hot spots' resulting from landfilled unidentified chemical wastes. The river discharges at a rate of 7000 m^3/s making it the largest source of materials into Lake Ontario (Mudroch 1983). This discharge rate is ten times the Connecticut River discharge rate and over three times the Chesapeake Bay estuary discharge rate.

Because of its larger surface to volume ratio Lake Erie's water temperature exhibits a greater response to surface heating and cooling than Lake Ontario's water temperature. The river water temperature changes little during its passage from Lake Erie to Lake Ontario resulting in a density difference between the river discharge and the ambient lake water. These temperature/density differences between the lake and the river outflow vary with season, such that in spring and fall the temperature in the Niagara River plume may be 3-4°C warmer than

the lake water, while in early summer and late fall the differences may vanish.

Figure 1.1 shows the bathymetry of Lake Ontario with an enlargement of the lake basin adjacent to the Niagara river mouth. The river is approximately 22 meters (m) deep at its mouth. Directly offshore the depth shallows to 5-10 m at the Niagara Bar. Offshore of the bar an outer shelf extends from the 10 m to the 20 m isobath. At the 20 m isobath, about 7 km offshore of the river mouth, the water depth drops from 20 to 70 meters in less than a kilometer. The shelf and slope, although of smaller scale, resemble a continental shelf and slope. Away from the river mouth the shelf width narrows to 3 kilometers (km).

Murthy et al. (1984) began a study of the Niagara River plume as part of a larger study investigating its relation to the coastal exchange between the near shore zone and the lake interior. They found that the thermal structure of the plume was complicated; however, a thermal front often formed at the edge of the Niagara Bar. This front was sharpest during the summer and fall. They also found the plume to be vertically mixed over the Niagara Bar, while offshore of the bar the plume spreads as a buoyant surface layer. Drogues released in the river mouth followed the plume with characteristic velocities of 20 cm/s away

from the mouth. On several occasions the drogues were trapped in nearshore eddies with scales of 1-2 km.

In addition to the temperature contrast between the Niagara River Plume and Lake Ontario water, the plume is often turbid such that the edge of the plume can be located by water color differences (Carey and Fox 1987). The color line associated with fronts has been well documented in a variety of fronts (e.g. Federov 1986). The plume can be identified in satellite images of suspended sediments and/or temperature throughout most of the year. Figure 1.2 shows the temperature signature of the plume in a thermal image taken by satellite. Aerial photographs taken during spring thaw show chunks of ice trapped along the edge of the plume.

The focus of this report is on the dynamics of the thermal front. This study examines the seasonal variability of the Niagara River plume and fronts. The analysis is based on some of the temperature and Lagrangian velocity data collected in the study by Murthy et al. (1984). The paper is divided into five sections. The first section being the introduction followed by (2) a description of the data, (3) the results of the experiments, (4) a discussion of the results and (5) the concluding remarks.

2. The Data Set

Temperature and velocity data were collected during seven experiments, of three to five day length between April 14 and November 11, 1982. The dates are listed in table 2.1.

Table 2.1. The dates of the temperature surveys and drogue experiments for the 1982 Niagara River plume study.

No.	Month	Days	Total Days
I	April	14-15	3
II	May	26-28	3
III	June	21-25,	5
IV	July	7-9,	3
V	August	10-12	3
VI	October	5-7	3
VII	November	8-10	3

A summary of the data collection methods is given here, more details can be found in Murthy et al. (1984). The study area, shown in figure 1.1, was a 10 x 10 km square, rotated 15° counter-clockwise from true north, with one side centered on the river mouth. The square was gridded by 500 m intervals in both the alongshore and offshore directions. Temperature sampling stations were designated at each grid intersection (over water) (figure 2.1).

Temperature profiles were measured using an electronic bathythermograph (EBT) and recorded on a strip chart recorder.

There was one temperature survey per day. Usually each survey began with a temperature profile taken at the river mouth. Then the ship proceeded offshore collecting profiles at selected stations until the water color and/or the temperature profiles indicated that open lake water had been reached. If possible, profiles were collected at stations bordering along the plume edge. Sometimes the coastal waters had the same temperature and optical properties as the plume water. Murthy et al. (1984) attributed this to strong mixing between the Niagara River discharge and well mixed coastal waters, some of which are mixed with Lake Erie water from the outflow of the Welland Canal.

The motion field of the river plume was measured using Lagrangian drogues. The drogues had a minimum depth of 3.5 m. During each temperature survey approximately ten drogues were released in the plume mouth and then were tracked by ship. Drogue tracking was limited to the 10 x 10 km study area. In the early experiments the drogues were released about one and half kilometers upstream of the river mouth, it was found they would converge on the eastern side of the mouth, thus the flow on the western side of the mouth was not represented. Later, in August and November, the drogues were released in a line across the mouth. In October the drogues were released in a line 500 m offshore of the mouth.

Originally the temperature data was digitized using the 9-point digitization scheme of NWRI; however, it was found that this scheme did not account for the details of the profiles at the plume edge. These profiles were redigitized electronically. The profiles were smoothed by fitting a cubic spline to the data. Water density was computed from the smoothed temperature data using an algorithm derived from Fine and Millero's (1973) equation of state (Bennett 1976).

3. Results

In this section the results of the temperature surveys are reviewed. The data is presented as density in sigma-t units (σ_t) defined $\sigma_t=(\rho-1)*1000.$, where ρ is the water density in g/cm^3. Density is preferred because of its dynamical significance, that is, the density gradients drive the horizontal pressure gradients. Temperature is not linearly related to density. In particular, near 4^oC is the maximum density of fresh water. Temperatures below 4^oC decrease in density, and so do temperatures above 4^oC; therefore, it is easier to interpret dynamics from the density scale.

Along the southern shore of Lake Ontario there is a persistent eastward current. The current is driven by the predominant westerly winds in the area and internal kelvin waves which propagate counter clockwise around the lake's perimeter. These eastward currents have been shown to reverse and flow

westward during strong easterly winds (Simons and Schertzer 1985). The alongshore directions will be defined in the sense of the propagation of Kelvin waves, that is, alongshore to the east is defined as downstream and alongshore to the west is defined as upstream.

The digitized and smoothed density data in sigma-t units are presented in two formats. In one the surface densities collected during each survey are gridded and contoured to create a horizontal surface density plot. The coastline and distance scale is drawn on each figure. This is important because the alongshore and the offshore boundaries of each contour plot vary as the area covered by each survey varies. The scale along the upstream boundary in each plot is the distance in kilometers from the shoreline border of the 10 x 10 km grid, and the scale along the onshore boundary is distance in kilometers from the upstream border of the grid (figure 2.1).

In the other format the density profiles collected along a grid line, in either the alongshore or offshore direction, during a survey were gridded and contoured to create a vertical temperature transect. The alongshore transects are numbered 1 through 21 starting at the onshore border of the survey grid and ending with transect 21 along the offshore border of the survey grid, 10 km offshore. The across-shore transects are numbered starting with transect 1 at the upstream border and ending with transect 21 at the downstream border (figure 2.1). The beginning

and end of each transect depends on the location of the profiles on the grid line. Along the top horizontal axis on each transect contour plot profile station numbers mark the profiles used to make the contour. Along the bottom axis is the alongshore distance in kilometers.

The temperature/density survey data is discussed by experiment. The July experiment has been omitted because of poor resolution of the plume features. The velocity data has been reported in Murthy et al. (1984); therefore, after the short summary in the following subsection, the results will be used only when needed to support the temperature/density surveys.

The Drogue data

The drogues were too deep to resolve the motion field at the frontal zone. Nevertheless, the drogue data provide useful information on the motion field within the the plume. Instead of showing all the results of the drogue experiments, we will use the data collected June 21 as an example of the typical plume motion field in the absence of wind forcing (figure 3.1). Ten drogues were released at the river mouth and initially moved offshore with speeds of 150 cm/s. As the drogues moved offshore they slowed and turned right. Away from the river mouth the drogues on the outside of the turning region traveled with speeds near 20 cm/s, while inside the turning region the drogue speeds were slower. The innermost drogues exhibit a tendency to turn

shoreward. Sometimes the drogues were trapped in an eddy over the Niagara Bar. A common location of these eddies is marked with an E in figure 3.1. The drogue experiments of November are shown later in this section.

The Temperature/Density Surveys

April 14-16

During the April experiment the water temperature was near freezing, ranging from 0.8 - 2.2°C. The river water was the colder, yet lighter than the ambient lake water. Floating ice was observed in and around the river mouth and adjacent coastline. The harsh winter conditions limited the surveys to within 5 km of shore.

The April 14 survey covers the area offshore and downstream of the river mouth. The surface density contours in figure 3.2 outline the plume as it moves offshore and downstream. The horizontal gradients are weak varying a total of 0.1 σ_t. The water is vertically mixed over most of the surveyed area as shown by the alongshore transect 10, located 4.5 km offshore of the mouth (figure 3.3). Station 207 is directly offshore of the river mouth. The lightest water (-0.1 σ_t) is shifted to the right (downstream) of river mouth. Farther downstream lighter water is spreading over heavier water.

The April 15 survey covers the area to the left (upstream) of the river mouth. During this survey many of the stations were

repeated, with a time difference between the first and second sampling of approximately 3 hours. The surface density contoured in figure 3.4a is a combination of all the stations sampled April 15, using in the case of duplicates, the first profile collected. Figure 3.4b uses all the stations surveyed, but this time in the case of duplicates the second profile collected is used. The two surface contour are similar with strong gradients defining the upstream edge of the plume. In figure 3.4a the plume appears to have spread upstream and offshore from the day before. Approximately 3 hours later, figure 3.4b shows the plume has moved offshore and upstream by a half a kilometer, giving 4.9 cm/s as a rough estimate of the frontal propagation speed. The Langragian velocities measured by the drogues in the plume were 20 cm/s, but directed parallel to the front.

By April 16 the horizontal surface density gradient had disappeared. The surface was nearly isothermal, and like the two previous days the water was vertically homogeneous. Winds during this three day experiment were weak. Starting on April 13 the winds blew from the northeast. Over the next few days the winds rotated clockwise blowing from northeast to east to west to northeast again.

May 27-28

In May the river discharge is denser than the surrounding surface water of the lake. Yet the surface density contours for

May 27 and May 28 show strong horizontal gradients or fronts, outlining the plume (figure 3.5). These density gradients along the front are stronger than those observed in April. On both days the plumes have approximately the same dimensions with the offshore extent of about 5.5 kilometers and a surface area within the survey grid of 40 km^2.

The May 27 alongshore transect 4, located 1.5 km offshore is shown in figure 3.6a. At the deepest part of the cross-section, just offshore of the Niagara River mouth, the water is vertically mixed. Downstream of the mixed region lighter water defined by the -0.1 σ_t (7.5^{o}C) isopycnal spreads out over colder heavier water; however, the resulting density gradients are too weak to be considered a front. Upstream the -0.1 σ_t water spreads under lighter, warmer water, until near station 2 where the -0.1 σ_t layer meets the pycnocline of the stratified coastal water. Near station 2 the isopycnals defining the lighter coastal water surface and form a front.

A clearer view of the front is shown in offshore transect 11 (figure 3.6b). Transect 11 starts at the river mouth (station 198), cuts across the Niagara Bar and the outer shelf and ends in open lake water. The river plume is vertically mixed over the Niagara Bar. At the edge of the bar the plume water (-.1 to -.14 σ_t) meets the stratified open lake water. The stratified open lake water has a seasonal pycnocline at 5 - 7 meters. Above the seasonal pycnocline, the surface layer is 0.1 σ_t lighter than the

plume water. A strong front forms where the surface layer meets the mixed plume water. The frontal characteristics are similar to those described by Garvine and Monk (1974), in that the horizontal density gradients are strong at the leading edge of the frontal layer - the lake surface layer - and the frontal layer deepens at the front. The deepening is due to downward vertical velocities and the subsequent entrainment of heavier water from below. In this case the heavier water is the plume water. Plume water is also mixing at the thermocline. The transverse density gradients located where the plume water meets the thermocline can drive a baroclinic circulation forcing the plume water to flow along the thermocline (Fischer et al. 1979).

June 21-25

In June the density contrasts are larger than observed in April and May. On average, during the June experiment, the Niagara River water is 0.4 σ_t lighter than the lake surface water. In figure 3.7 the surface density contours are shown for the five days of the experiment. The contour interval in the surface density plots has been changed from 0.02 σ_t, used for April and May, to 0.05 σ_t.

June 21, figure 3.7a, the river plume is defined by weak density gradients. In the figure isopycnals move offshore from the coast, turn right and follow the coast downstream. The next day, June 22, the density gradients have strengthened, forming a

front upstream and offshore of the mouth. On June 23 the plume front is closer to the mouth than on the day before. For example, on June 22 the plume extends approximately 8.5 km offshore, while on June 23 the plume extends 7 km offshore. Also, the river discharge has warmed from 15.2° C (-.91 σ_t) on June 22 to 15.7° C (-.98 σ_t) on June 23.

There is an abrupt change in the surface density contours on June 24. Water lighter (warmer) than the river water is upstream and downstream of the river mouth, with the upstream density gradients strong enough to form a front. A density front separating lighter plume water from heavier lake water is 8.5 km offshore. Within a day the anomalous lighter water disappears and the plume resumes its previous shape. The June 25 plume extends about 7 km offshore and is bounded by strong horizontal density gradients along the upstream and offshore borders. The density gradients weaken downstream following the plume front.

The changing vertical structure of the Niagara River plume is shown by comparing offshore transect 11 over four days, June 22 - 25 (figure 3.8). The seasonal pycnocline of the lake, centered about the -.25 σ_t isopycnal, is located just below the outer shelf edge in transect 11. In each transect the plume is vertically homogeneous over the Niagara Bar, and at the offshore edge of the bar the lighter river plume water separates from the bottom and flows out over heavier lake water forming a sharp front between the plume water and the lake water.

On June 22 the plume is the farthest offshore of the four days. The plume is less than a meter at its leading edge. The surface front is likely to be smeared since the stations are 500 m apart. The next day, June 23, the front is closer to shore. The density gradients between the plume and the lake water are weaker, while the seasonal thermocline is sharper. The plume is deeper and the isopycnals are nearly vertical at the leading edge of the front.

On June 24, the date with the atypical surface density, the plume isopycnals have merged with the thermocline isopycnals. The resulting gradients are weak implying mixing between the plume, the lake surface water and the thermocline. The deepening isopycnals below the buoyant layer suggest that lake water is being entrained into the plume from below. An additional station was taken between stations 214 and 215, where a sharp color line, distinguishing plume water from open lake water, was observed.

The June 25 plume is the closest inshore and nearly vertically homogeneous. The isopycnals defining the plume have a steep slope at the offshore edge of the shelf.

The June 24 and 25 alongshore transects 11, located 5 kilometers offshore, is shown in figure 3.9. These transects emphasize that a complete change in structure can occur in one day. Station 208 on each transects marks the station directly offshore of the river mouth. On both days the plume is well mixed over the shallow water of the Niagara Bar. Upstream, on

June 24, the vertically mixed river discharge is bounded by stratified coastal water. The river plume is the same density as the thermocline of the coastal water. Similar to the observations in May a front forms at where the lighter surface layer spreads out over the heavier river plume water. Downstream, on June 24, a layer of warmer (lighter) water floats on the river plume; however, no distinct front exists, only a gradual change in density (temperature). The lighter surface water downstream did not prevent the drogues from flowing downstream. The following day, June 25, the water is vertically mixed offshore of the mouth (station 208) and downstream. A barotropic front has formed at the upstream boundary of the river discharge plume. The front is between stations 167 and 187. Upstream of the front the vertical isopycnals imply a quick shelf response to wind mixing.

August 11-12

The surface density contours for August 11 and 12 are compared in figure 3.10. On August 11 the upstream edge of the plume is defined by strong density gradients. The river water density at the mouth is -2.30 σ_t (22.4^{o}C) and the maximum surface density surveyed is -1.90 σ_t (20.6^{o}C). The next day, August 12, the upstream front has disappeared. The nearshore surface density contrast are weak density contrasts, with lighter (warmer) surface water downstream of the mouth. Offshore a weak

front exists between the river plume water and heavier lake surface water. For each of the two days offshore transect 11 is plotted in figure 3.11. On August 11 the river discharge is completely mixed from the river mouth to the edge of the Niagara Bar, where the river discharge plume separates from the bottom and spreads offshore as a buoyant layer. The buoyant layer is deep with vertical isopycnals at the leading edge. Because the profiles were taken 1 km apart the surface front is smeared. August 12 the plume is gone. The -2.25 σ_t isopycnal defining the plume water extends down to the sharp seasonal pycnocline. The fate of the plume on August 12 is clarified in alongshore transects 8 and 16, located 3.5 and 7.5 kilometers offshore (figure 3.12). In transect 8 the river plume is vertically mixed over the bar. Upstream the plume spreads out over the surface of the heavier shelf water. Downstream the plume is bounded by stratified shelf water. In transect 16, located 4 km offshore of the shelfbreak, the intense seasonal pycnocline dominates the density field. Upstream of the mouth, left of station 213, the river plume (defined by the -2.25 σ_t isopycnal) is a thin buoyant layer at the surface. Near station 213 the plume deepens sharply. The vertical isopycnals imply strong mixing in the deepened surface layer. Farther downstream the -2.25 σ_t plume water is thick layer sandwiched between the lighter surface warmed water and the seasonal pycnocline.

Strong westerly wind dominated August 7 through 11. Starting early August 12 the winds reversed and blew at 3-4 m/s from the east. The easterly wind may have driven the lighter plume water upstream and offshore. The upwelling favorable wind is likely to have increased mixing in the upper layer.

October 5-7

During the October experiments thorough surveys of the 10 x 10 km grid were completed. Easterly winds of 2-4 m/s blew from October 3 to 7. Each of the surface density contours for October 5, 6, and 7 shows a strong front defining the upstream and offshore boundary of the plume (figure 3.13). The front extends beyond the offshore edge of the survey grid. The plume water, defined by the -1.25 σ_t (17.3°C) isopycnal, is lighter than the surrounding shelf surface water of -.90 σ_t (15.2°C). Towards the downstream inshore corner of the survey grid the surface water gradually cools (becomes heavier). Over the three days, the density gradients bordering the plume tighten, strengthening the front. The plume front moves downstream and inshore with time.

The three-dimensional features of the plume are similar over the three day experiment; therefore, the alongshore and offshore transects collected on October 5 will be used as an example. The alongshore transects 8, 14, and 20, located 3.5, 6.5, and 9.5 kilometers offshore, are plotted in figure 3.14. Nearshore

(transect 8) the river plume water is mixed over the Niagara Bar. Upstream and downstream of the bar the lighter river plume water spreads out over the surface of the heavier coastal lake water. Upstream the density contrast separating the buoyant plume layer from the coastal water is sharp relative to the same density contrast downstream. Over the edge of the outer shelf (transect 14) the buoyant plume water has separated from the bottom. In this plot station 211 marks the position directly offshore of the river mouth. The plume is deepest just downstream of station 211. Farther downstream the plume water mixes with the lake water weakening the density gradients defining the plume and cooling the plume water as it moves downstream. The plume spreads and thins upstream, while the density gradients defining the plume stay strong. Over open lake water (transect 20) the plume is a thin surface layer. The isopycnals defining the plume are slanted down to the right, such that the plume is thickest downstream and upstream the plume front intersects the surface upstream. Below the plume is the seasonal pycnocline, which has weakened considerably since August.

Three offshore transects are shown in figure 3.15. In transect 3, 4 kilometers upstream of the river mouth, the plume is a thin layer, less than 5 m deep, extending from shore to the edge of the shelf break. The plume ends with a sharp front at its leading edge. Transect 11, starting at the river mouth, shows the plume well mixed over the Niagara Bar. After the bar,

at the beginning of the outer shelf the plume separates from the bottom and spreads offshore, thinning as it spreads. The plume separates from the bottom offshore of its usual position at the edge of the bar. Two kilometers downstream of transect 11, transect 15 shows the plume has almost completely separated from the bottom. The plume is deepest at its center over the shelfbreak. The isopycnals rise on either side of the plume center. The plume front weakens offshore as the plume mixes with lake water. To maintain a geostrophic balance, the slope of the isopycnals near the coast requires a baroclinic flow upstream, while the slope of the plume front isopycnals offshore requires a downstream flow. The opposing flows may be responsible for the semi-permanent eddy found in this area (Murthy, Miners and Sandall 1987)

November 8-10: Wind reversal

The November surveys are unique in that they document a wind reversal. The surface density contour plots for November 8, 9, and 10 are plotted next to the Lagrangian drogue velocities collected on the same days (figures 3.16, 3.17, and 3.18). Included on each figure is a stick plot of the local wind velocity from November 6 to 10. The drogue movements illustrate that the surface density field is strongly linked to the horizontal motion field driven by the wind.

The average density contrast between the Niagara River discharge and the ambient lake water for the November experiments is .16 σ_t, a smaller density difference than measured in June, August, and October. The contour interval in the figures is now 0.02 σ_t, the same interval used in May and April.

On November 8 the winds were strong and from the west. The plume, defined by a front along its upstream and offshore sides, is within four kilometers of shore, thus, confined to the area over the Niagara Bar. Alongshore and offshore transects show the water column is vertically mixed and the front is barotropic, that is, the isopycnals defining the front are vertical, top to bottom. The drogues move offshore at the mouth, and turn right following along the plume outline. Drogue speeds are initially around 150 cm/s and slow to an average speed of 20 cm/s.

Early November 9 the winds are 5-6 m/s from the southwest then shift to the northwest and weaken to 2-3 m/s. This wind action effectively relaxes the alongshore component of the wind. The alongshore component of the wind drives the alongshore currents in Lake Ontario (Simons and Schertzer 1985). The plume responds by spreading offshore and upstream. On November 9 the plume is approximately 6 km offshore. The drogues begin to follow the plume by starting offshore and then turn downstream over deep water. The offshore transect 11 shows a strong plume front defined by isopycnals sloping upward and offshore from the edge of the Niagara Bar (figure 3.19).

November 10 the winds strong (7-8 m/s) from the east. The plume boundaries are less distinct in the surface density plot (figure 3.18). The lighter plume water ($\approx -.28\ \sigma_t$) is upstream and offshore, coinciding with the movement of the drogues. The offshore transect 11 shows the plume boundary is diffuse, a result of mixing with the seasonal pycnocline and the lake surface layer.

4. Discussion

General Plume Characteristics

The size and the shape of the Niagara River plume varies; however, the typical plume flows offshore from the river mouth, turns right and flows downstream. The plume is usually bounded by strong horizontal density gradients or fronts. Over the Niagara Bar the plume is vertically homogeneous, and often at the edge of the bar the buoyant plume separates from the bottom and spreads offshore. The offshore extent of the plume appears to be strongly related to wind forcing. The temperature surveys were limited to a 10 x 10 km grid adjacent to the river mouth; however, the plume frequently extended beyond the offshore and downstream grid boundaries. Within the grid the surface area of the plume was close to 50 km^2.

Some of the plume's features such as; the stability of the plume and the strength of the plume fronts, are related to the buoyancy of the river relative to the ambient lake water. For

example, small density differences between the river and the lake result weak density fronts, thus, enhanced mixing between the two by wind action. While the volume flux of the Niagara River into Lake Ontario is constant throughout the year, the river's buoyancy flux into the lake exhibits strong seasonal variations. Fischer et al. (1979) defines the specific buoyancy flux, B, as

$$B = g'Q, \tag{4.1}$$

where

$$g' = g\frac{(\rho - \rho_o)}{\rho_o} \tag{4.2}$$

is the reduced gravity, ρ is the river water density, ρ_o is the ambient lake water density, g is the gravitational acceleration and Q is the specific volume flux. The buoyancy flux during each experiment is plotted in figure 4.1. In May the buoyancy flux was negative due to the river water being heavier than the lake surface water. The smallest positive buoyancy inputs were during April and November, the first and last experiments, and the largest buoyancy input was in October.

The dynamics of the plume are governed by a balance between buoyancy, momentum, and Coriolis effects. Over the Niagara Bar where the flow is vertically mixed, the flow is strongly non-linear and dominated by momentum. Because of the surface and bottom boundaries the plume over the bar must mix by lateral

entrainment. Over the bar the flow is further complicated by topographic effects and the influence of bottom friction. The importance of the earth's rotation on the motion field can be estimated by the Rossby number (R_o), defined by $R_o = U/fL$, where U is the characteristic fluid velocity, f the Coriolis parameter and L the characteristic length scale. For geostrophic motion to be important the Rossby number is small. Near the river mouth, U is 1.5 m/s, f is $10^{-4}s^{-1}$, and L is 1 km, the river mouth width, resulting in R_o equals 10; therefore, nonlinear motion dominates. As the plume moves offshore and spreads the fluid velocity slows and the length scale increases, thus, R_o decreases.

At the edge of the bar the plume separates from the bottom as buoyancy becomes important. Here R_o is 0.5 and Coriolis effects become evident, turning the flow right along the upward sloping isopycnals as the plume spreads offshore.

In a non-rotating system, the buoyancy forces translate into a horizontal radial pressure gradient which acts uniformly in all directions, spreading the buoyant surface layer away from its source. The earth's rotation adds a lateral flow making the plume and the associated fronts more complicated. One parameter to estimate the influence of the earth's rotation on the buoyant flow is the Kelvin number (Ke) - the ratio of the geomorphology, the river mouth width, to the internal Rossby radius. The internal Rossby radius is $R_i = f^{-1}(g'h)^{1/2}$ where h is the water

depth. Using the April to November, 1982 data, R_i for the Niagara River plume ranges from .7 to 2 kilometers (figure 4.2). Thus, the Kelvin number is order one, resulting in strong Coriolis action on the plume.

Chao and Boicourt (1986) use a primitive equation model to examine a buoyant plume in a rotating system. Their model releases buoyant water from a narrow estuary perpendicular to the coast into a deep homogeneous ocean. The plume spreads offshore and executes an anticyclonic turn. As the plume turns and approaches the coast the flow forms a coastal current, roughly one internal Rossby radius wide, running parallel to shore with the coast on the right. The results of Chao and Boicourt (1986) look similar to the satellite image of the Niagara River plume in figure 1.2. Just offshore of the mouth, over the Niagara Bar there is a large bulge in the image, the anticyclonic turning region, followed by a narrow coastal current. The bulge is located approximately over the Niagara Bar. Chao and Boicourt (1986) predict strong mixing driven by vertical velocities in the turning region, consistent with the vertical homogeneity of the plume over the Niagara Bar. In a follow-up paper Chao (1988) ran the model with constant wind forcing. Downwelling favorable winds, blowing with the coast to the right forced the buoyant plume along the right hand coast, intensifying the coastal current. Upwelling favorable winds cause an offshore excursion of the plume, and significantly weaken the stratification,

thereby, weakening the development of a coastal current. These results simulate the results of the November experiment when the winds switched from downwelling favorable to upwelling favorable over a three-day period.

General Front Characteristics

Two types of dynamically different fronts are found bordering the Niagara River plume. Although they appear identical in the surface density plots, they are easily identified in the vertical transects. One front is found at the leading edge of the plume's buoyant spreading layer and is similar to the front described by Garvine and Monk (1974). This type of front will be called a buoyant plume front. The other front is often observed at the upstream border between the vertically mixed plume and the stratified shelf water. This front is much like the coastal front of Simpson and Hunter (1974) and, thus, will be called a coastal front.

An illustration of the buoyant plume front taken from Federov (1986) is shown in figure 4.3. The velocity arrows in the figure represent the motion relative to the front. As the front spreads offshore the heavier ambient water appears to move under the front, while at the surface of the frontal layer the horizontal pressure gradient resulting from the buoyancy forces drive the flow toward the front. This convergent motion drives

downward vertical velocities entraining the heavier ambient water from below into the plume.

Often these fronts are found along the offshore border of the Niagara River plume; therefore, the plume is diluted by entraining lake water into the plume. In May the surface water of the lake is lighter than the river water causing the river discharge plume to sink below the lake surface water. The buoyant lake surface water is now the frontal layer and the heavier plume water is entrained upward into the lake surface water. An example of this is shown in figure 3.6.

The coastal front was described by Simpson and Hunter (1974) using observations of fronts in the Irish sea. They found that over much of the Irish sea shelf tidal stirring is strong enough to maintain a vertically homogeneous water column, while in deeper water lower levels of tidal stirring permit stratification. This results in the shelf being partitioned into mixed coastal shelf water and stratified water over deeper areas of the shelf separated by sharp frontal zones. Simpson and Hunter (1974) propose that the balance between stirring and heating (stratification) can be represented by the parameter $\phi h/U^3$ = constant , where ϕ is the heating rate, h is the water depth and U is the mean depth tidal velocity. Since ϕ is usually constant over scales considered here, their frontal parameter is simplified to h/U^3. Simpson and Hunter (1974) that maintain coastal fronts occur at some constant value for h/U^3. An example

of a coastal front, taken from Federov (1986) is shown in figure 4.4.

Fronts similar to the coastal front are observed along the upstream boundary of the Niagara River plume. Instead of tidal stirring the mixing is provided by the high plume velocities near the river mouth. In figure 3.9a there is a fine example of this type of front. In the center of the alongshore transect, directly offshore of the river mouth (station 204), the plume is vertically homogeneous, while 2 km upstream the shelf water is stratified. The front is located at the sharp transition between the two regions. The frontal zone is an area of strong velocity shear between the shelf water and the plume water. Strong lateral entrainment of shelf water into the plume is expected. This is supported by the satellite image in figure 1.2. The image shows coastal shelf water upstream of the river mouth being entrained and pulled offshore by the Niagara River plume.

The frontal dynamics are complicated by the influence of the earth's rotation adding a horizontal flow along the front. Garvine's (1987) model of estuary plumes and fronts explains some of the differences. He defines two types of fronts; a degenerate front and a depth discontinuity front. The depth discontinuity front is where the isopycnals undergo a finite depth change across the front, and the degenerate front is where the depth change is zero, such as when the upper layer vanishes smoothly. An example of a depth discontinuity front is given in figure 3.8b

and an example of a degenerate front is given in figure 3.14c. These differences are important dynamically. The depth discontinuity front will generate its own dynamic balance distinct from the buoyant layer dynamics as discussed above and in Garvine (1974b) and Kao et al. (1977), while the degenerate front will be mere streamlines.

The results of one of Garvine's (1987) model cases, which resembles the Niagara River plume, is shown in figure 4.5. In the model the buoyant discharge flows out of a channel perpendicular to the coast into a deep ocean. A uniform current flows alongshore with the coast to the right. The plume turns first by the action of the alongshore current and later (about 0.6 R_i downstream) by the Coriolis action. The bounding discharge front weakens from the depth discontinuity type to a degenerate front as the flow turns right and approaches the coast. The dashed line marked D=0 is where the plume depth goes to zero. Inshore of this line there is no flow. The discharge front intersects the coastal current front at approximately 3.7 R_i downstream of the mouth for order one Kelvin numbers. This model requires the plume flow to be supercritical, that is, the Froude number (q/c) is greater than one, where q is the fluid speed and $c=(g'h)^{1/2}$ is the internal phase speed.

Using the temperature surveys and the drogues velocities, the flow throughout the Niagara river plume was found to be supercritical, with the highest Froude numbers (close to 4) near

the upstream plume edge. The model plume simulates many of the features observed in the October transects. For example, offshore transect 3 in figure 3.15a shows the plume close to the river mouth bounded by a depth discontinuity type front at its leading edge, while away from the river mouth in alongshore transect 20 in figure 3.14c the front is the degenerate type. Two kilometers downstream of the mouth, transect 15 shows the offshore edge of the plume has thinned and weakened, typical of a degenerate type front (figure 3.15c). Inshore the isopycnals slope upward toward the coast similar to the model when the plume depth goes to zero (D=0). At D=0 the plume separates from the coast and a dead zone is created, which may explain the nearshore trapping of drogues in the Niagara River plume (figure 3.16).

5. Concluding Remarks

The fronts of the Niagara River plume are of critical importance to the mixing between the Niagara River and Lake Ontario. The exchange of waters at the frontal boundary may be one of the most important factors on determining how quickly a pollutant is dispersed. When the Niagara River discharge is less dense than the ambient lake water, the lake water is entrained into the plume. The plume, influenced by the earth's rotation, tends to turn and concentrate along the coast in a coastal current flowing parallel to shore with the coast to the right.

Thus, exchange between the open lake and the plume is limited. When the river discharge is buoyant the materials in the plume remain in the plume which concentrates along the coast.

Wind forcing can dissipate the plume depending on the buoyancy of the plume and the wind direction. Vertical mixing by the wind is inhibited by strong stratification. Upwelling favorable winds enhance dissipation of the plume by blowing the plume offshore weakening the density gradients. Downwelling favorable winds inhibit dissipation of the plume by concentrating the plume even more along the downwind coast.

Dissipation of the plume may also be caused by barotropic or baroclinic instabilities along the plume front. These features are recognized by waves along the frontal boundary or as eddies, resulting from frontal wave breaking, swirling plume and lake water together. Though these features were not examined here, a stability analysis is a natural extension of this work.

The importance of fronts on the exchange between the Niagara River and the lake warrants further investigation. The Niagara plume fronts should be examined on a small intensive scale to determine the mixing intensities of the various types of fronts discussed earlier. Also, the fronts should be examined on a large scale using aerial or satellite imaging to access their extent and persistence. Both studies need to be temporally intensive to examine the time scale of frontal variability.

Numerical modeling of the Niagara River plume is extremely difficult because of the turbulent nature of the plume over the Niagara Bar. A laboratory model may prove to be more fruitful. I suggest a three part approach to numerical modeling by breaking the model into parts and examining each part separately then patching them together. This approach has been successful in many modeling efforts, for example, the adding of boundary layers to interior flows. The parts would be (1) the Niagara Bar, (2) the buoyant plume, and (3) the Niagara plume front which varies from the coastal front to the depth discontinuity type to the degenerate type. A frontal model could clarify the nature and rate of the exchange between the Niagara River and Lake Ontario.

REFERENCES

Bennett, E.B., 1986. Calculated relationships among temperature, density, pressure, and depth useful for study of freshwater lakes. Unpublished manuscript. Canadian Center for Inland Waters, Burlington, Ont., Canada. 22 pp.

Boicourt, W.C., 1973. The circulation of water on the continental shelf from Chesapeake Bay to Cape Hatteras. Ph.D. dissertation, Johns Hopkins University, Baltimore, Md.

Carey, J.H. and M.E. Fox, 1987. Distribution of chlorinated benzenes in the Niagara River plume. National Water Res. Inst., Burlington, Ont., Canada, Contribution #87-86. 27 pp.

Chao, S.-Y., 1988. Wind-driven motion of estuarine plumes. J. Phys. Oceanogr., 18:72-88.

Chao, S.-Y., and W.C. Boicourt, 1988a. The onset of estuarine plumes. J. Phys. Oceanogr., 16:2137-2149.

Cordes, R.E., S. Pond, B.R. de Lange Boom and P.H. LeBlond, 1980. Estimates of entrainment in the Fraser River plume, British Columbia. Atmosphere-Ocean, 18:15-26.

Federov, K.N., 1986. *The Physical Nature and Structure of Oceanic Fronts.* Springer-Verlag, New York, 326 pp.

Fine, R.A. and F.J. Millero, 1973. Compressibilty of water as a function of temperature and pressure. J. Chem. Phys., 59:5529.

Fischer, H.B., E.J. List, R.C.Y. Koh, J. Imberger and N.H. Brooks, 1979. *Mixing in Inland and Coastal Waters.* Academic Press, Orlando, Fla., 483 pp.

Garvine, R.W., 1974a. Physical features of the Connecticut River outflow during high discharge. J. Geophys. Res., 79:831-846.

Garvine, R.W., 1974b. Dynamic of small-scale oceanic fronts. J. Phys. Oceanogr. 4:557-569.

Garvine, R.W., 1984. Radial spreading of buoyant, surface plumes in coastal waters. J. Geophys. Res., 89:1989-1996.

Garvine, R.W., 1977. Observations of the motion field of the Connecticut River plume. J. Geophys. Res., 82:441-454.

Garvine, R.W., 1987. Estuary plumes and fronts in shelf waters: a layer model. J. Phys. Oceanogr., 17:1877-1896.

Garvine, R.W. and J.D. Monk, 1974. Frontal structure of a river plume. J. Geophys. Res., 79:2251-2259.

Ingram, R.G., 1981. Characteristics of the Great Whale River plume. J. Geophys. Res., 86:2017-2023.

Kao, T.W., C. Park and H.-P. Pao, 1977. Buoyant surface discharge and small-scale oceanic fronts: a numerical study. J. Geophys. Res., 82:1747-1766.

Mudroch, A., 1983. Distribution of major elements on sediment cores from the western basin of Lake Ontario. J. Great Lakes Res., 9:125-132.

Murthy, C.R., D.C.L. Lam, T.J. Simons, J. Jedrasik, K.C. Miners, J.A. Bull and W.M. Schertzer, 1984. Dynamics of the Niagara River plume in Lake Ontario. National Water Res. Inst., Burlington, Ont., Canada, Contribution #84-7, 120 p.

Murthy, C.R., K.C. Miners, and J.E. Sandall, 1987. Mixing characteristics of the Niagara River plume in Lake Ontario. National Water Res. Inst., Burlington, Ont., Canada, Contribution #87-82, 16 pp.

O'Donnell, J., 1986. A numerical model of the dynamics of buoyant discharges. Ph.D. dissertation, University of Delaware, 182 pp.

Ryther, J.H., D.W. Menzel and N. Corwin, 1967. Influence of the Amazon River outflow on the ecology of the western tropical Atlantic. J. Mar. Res., 25:69-83.

Scarpace, F.L. and T. Green III, 1973. Dynamic surface temperature structure of thermal plumes. Water Resour. Res., 9:138-153.

Simons, T.J. and W.M. Schertzer, 1985. The circulation of Lake Ontario during the summer of 1982 and the winter of 1982/83. National Water Res. Inst., Burlington, Ont., Canada, Contribution #85-26, 116 p.

Simpson, J.H., and J.R. Hunter 1974. Fronts in the Irish Sea. Nature London, 250:404-406.

Wright, L.D. and J.M. Coleman, 1971. Effluent expansion and interfacial mixing in the presence of a salt wedge, Mississippi River delta, J. Geophys. Res., 76:8649-8661.

(a)

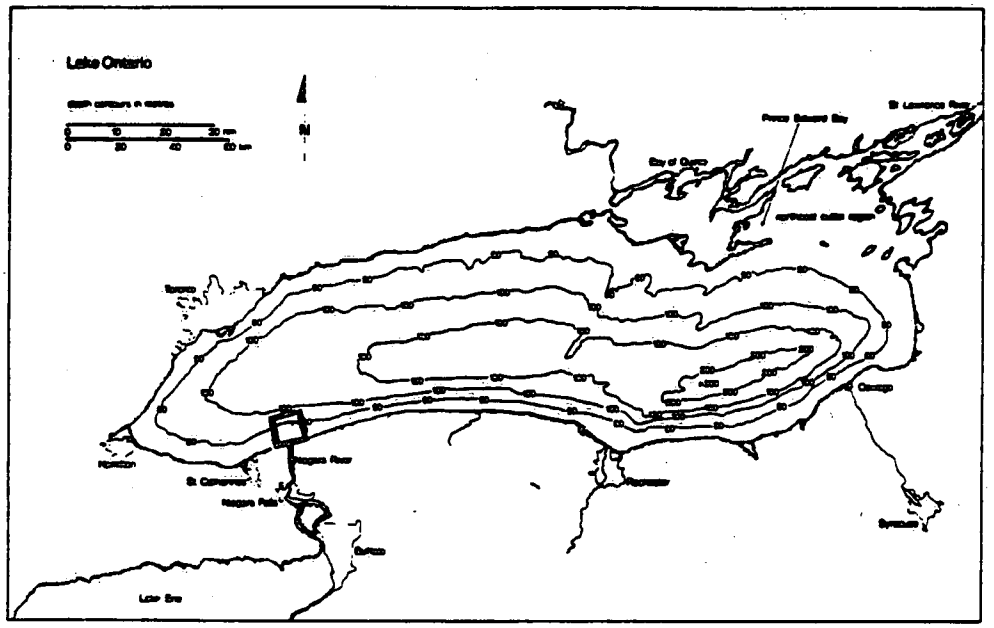

(b)

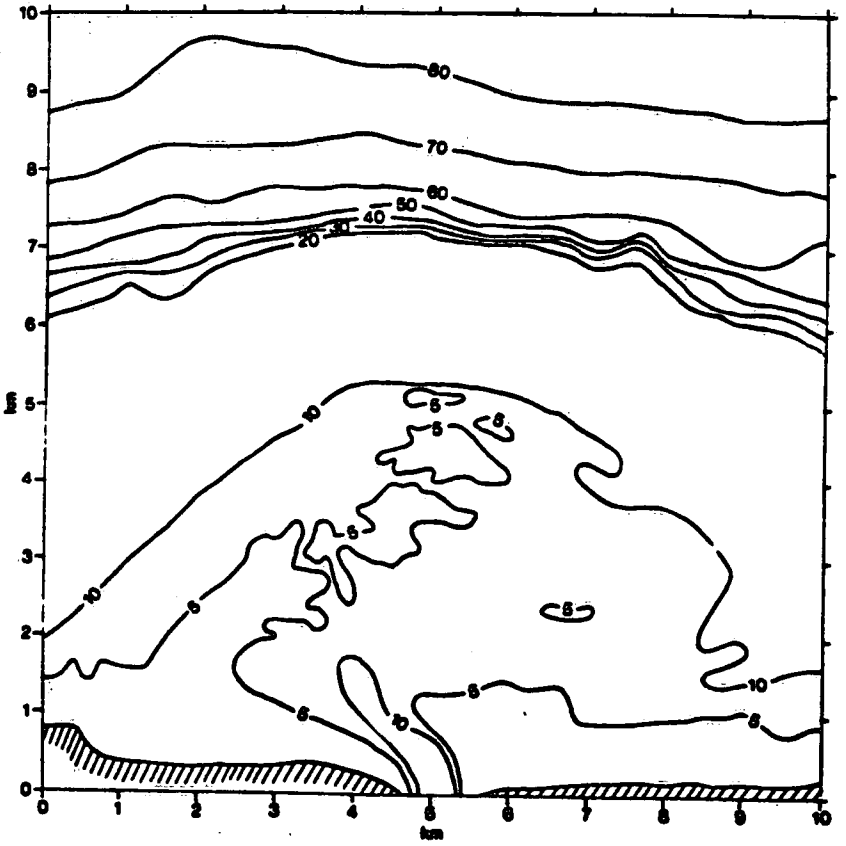

Figure 1.1

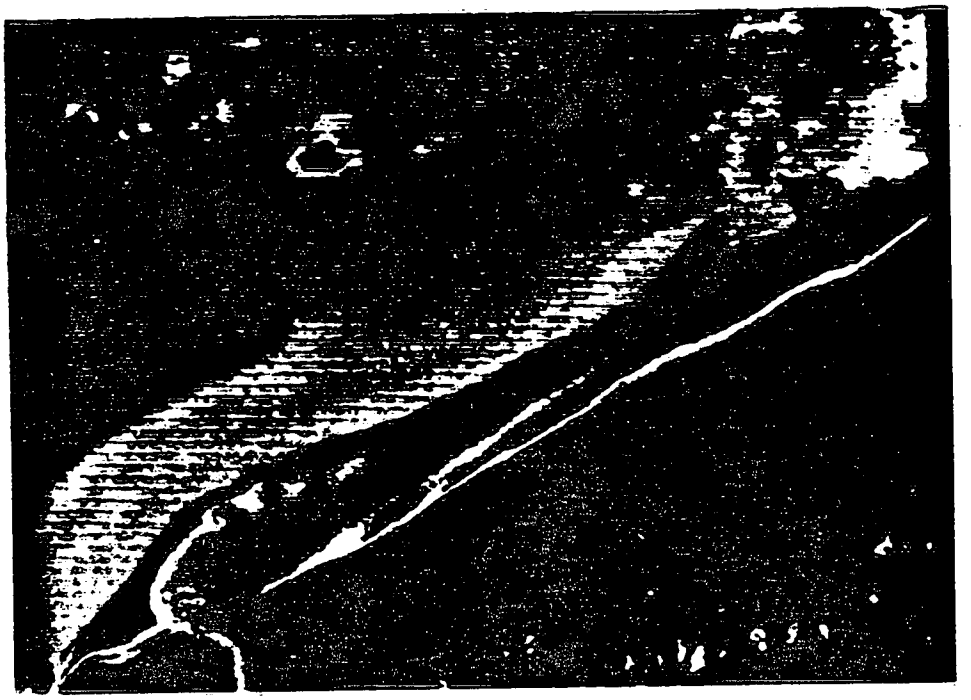

Figure 1.2

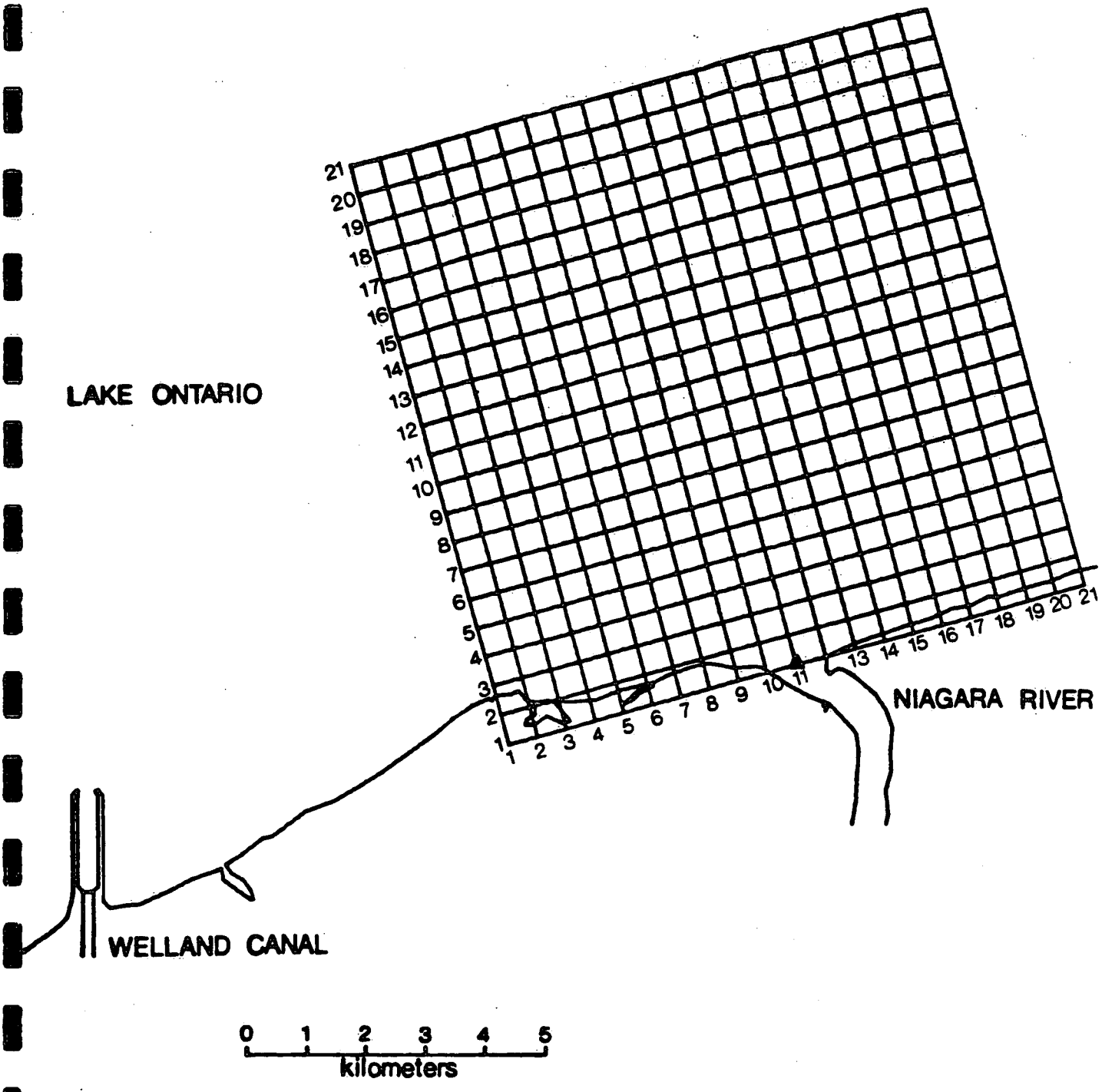
LAKE ONTARIO
NIAGARA RIVER
WELLAND CANAL
0 1 2 3 4 5
kilometers

Figure 2.1

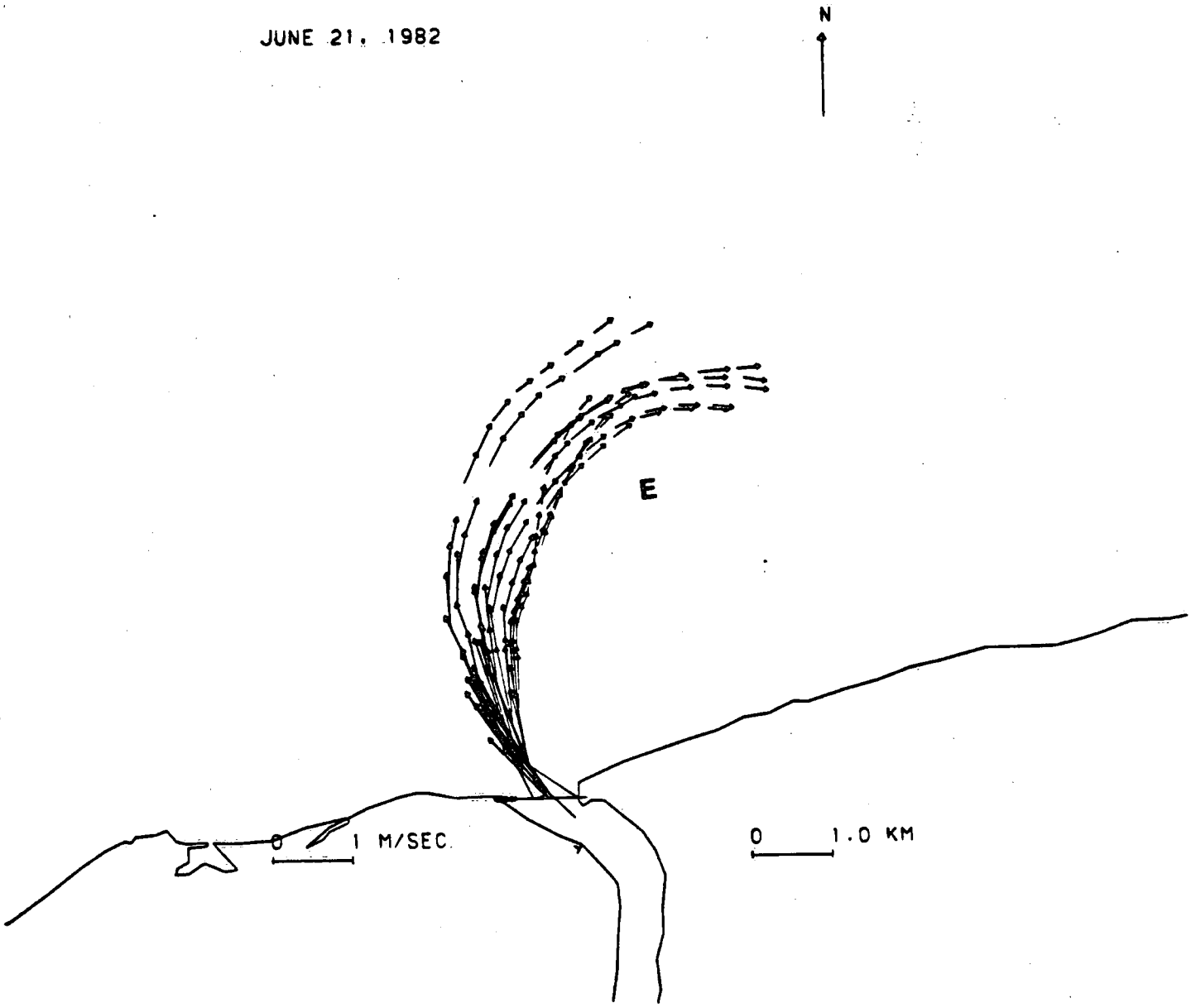

Figure 3.1

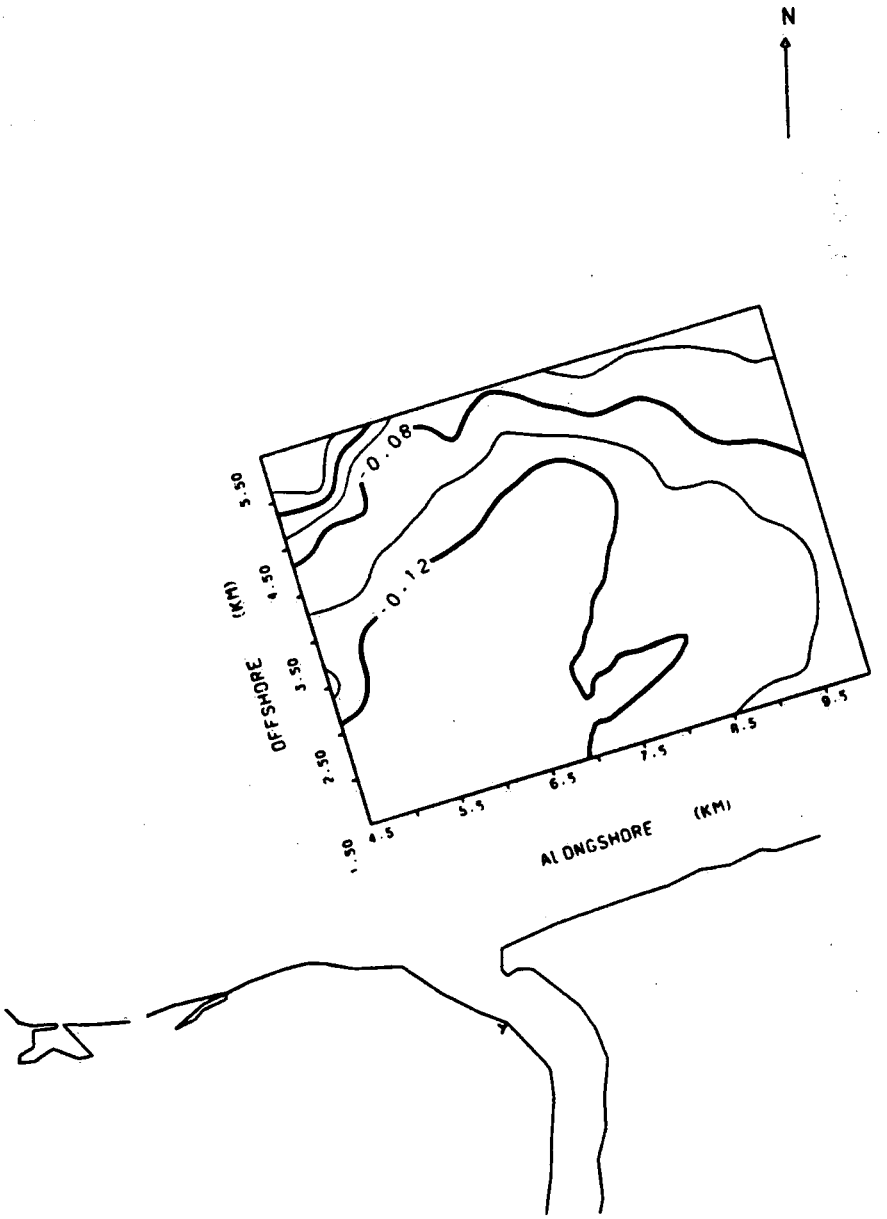
N
0.08
0.12
OFFSHORE (KM)
5.50
4.50
3.50
2.50
1.50
4.5
5.5
6.5
7.5
8.5
9.5
ALONGSHORE (KM)

Figure 3.2

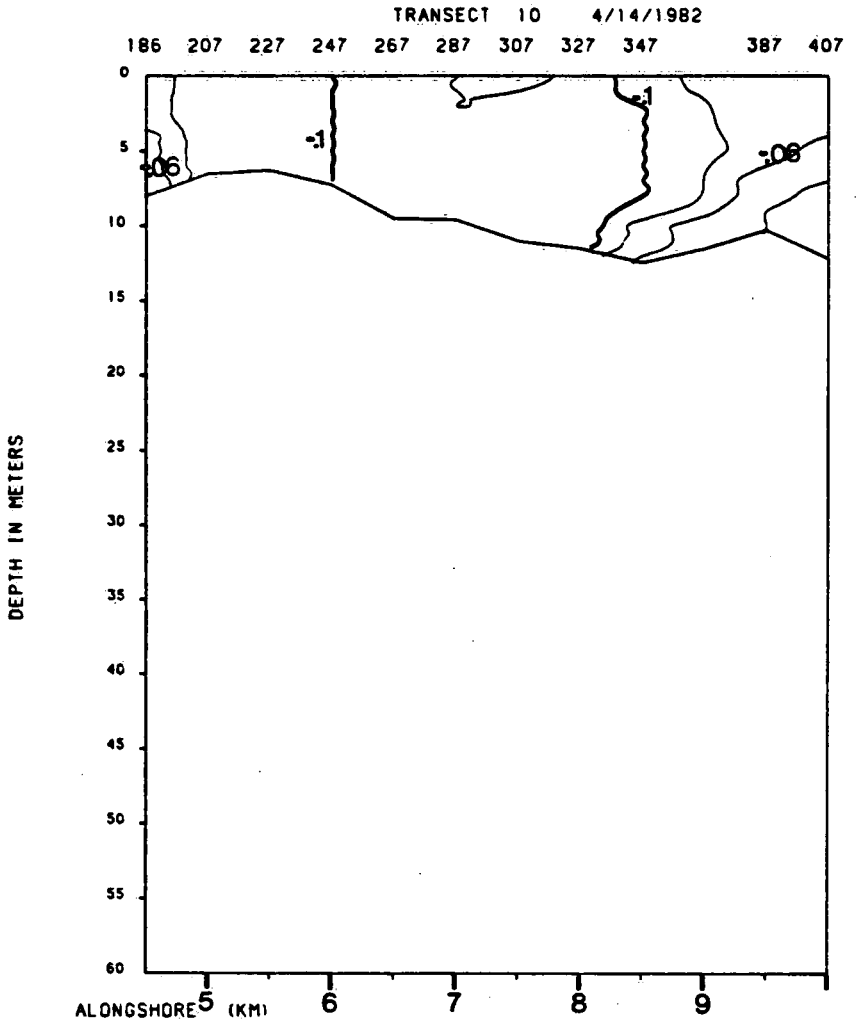
TRANSECT 10 4/14/1982
186 207 227 247 267 287 307 327 347 387 407
0
5
10
15
20
25
30
35
40
45
50
55
60
DEPTH IN METERS
-.1
-.1
-.06
-.08
ALONGSHORE 5 (KM) 6 7 8 9

Figure 3.3

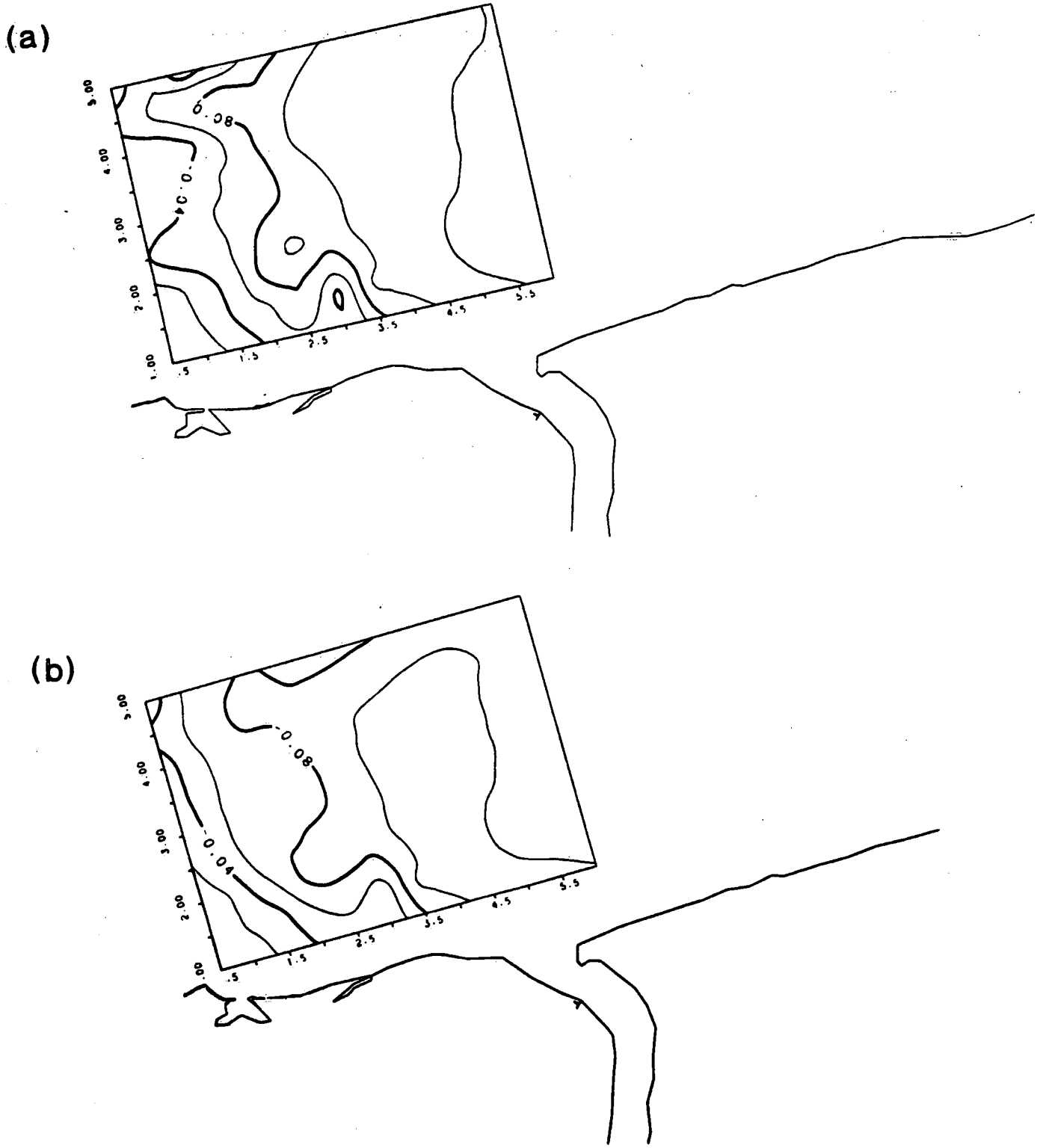

Figure 3.4

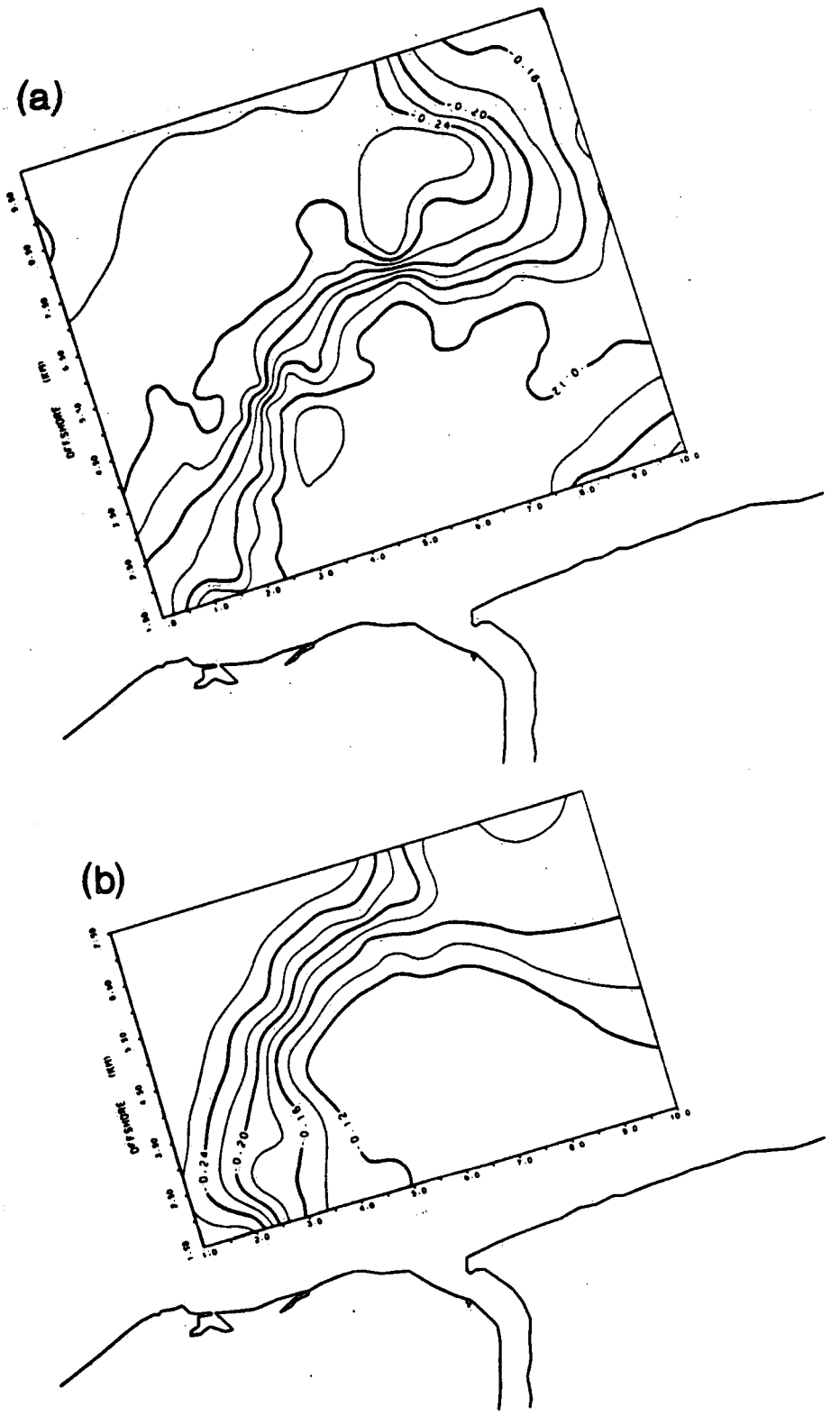

Figure 3.5

(a)

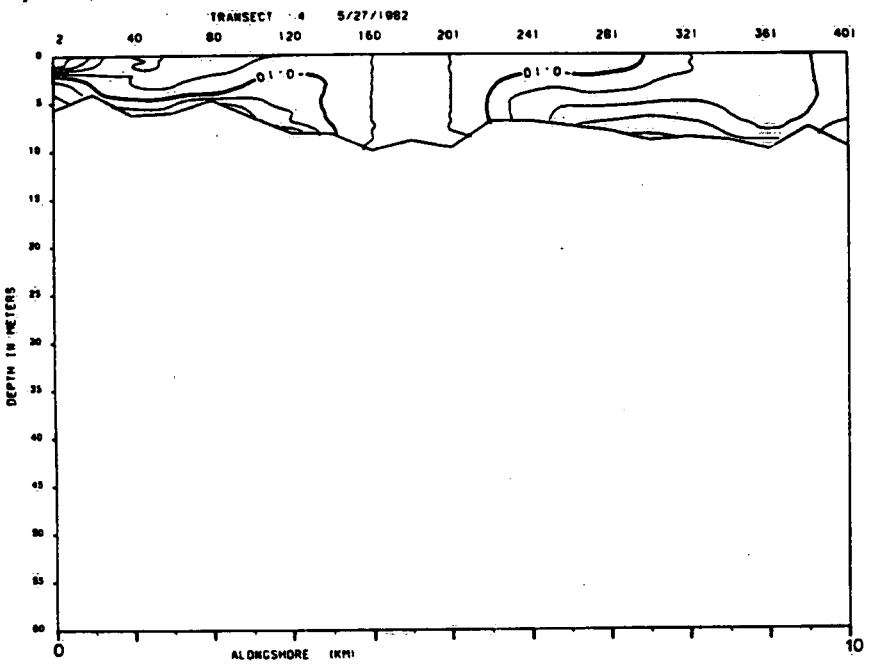
TRANSECT 4 5/27/1982
2 40 80 120 160 201 241 281 321 361 401
0.1 0
0.1 0
DEPTH IN METERS
0 5 10 15 20 25 30 35 40 45 50 55 60
0
ALONGSHORE (KM)
10

(b)

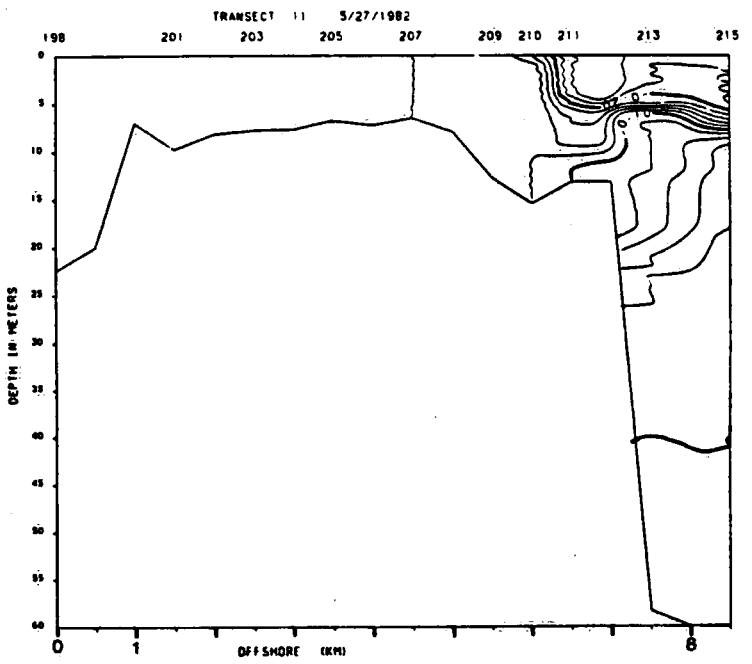
TRANSECT 11 5/27/1982
198 201 203 205 207 209 210 211 213 215
DEPTH IN METERS
0 5 10 15 20 25 30 35 40 45 50 55 60
0
1
OFFSHORE (KM)
8

Figure 3.6

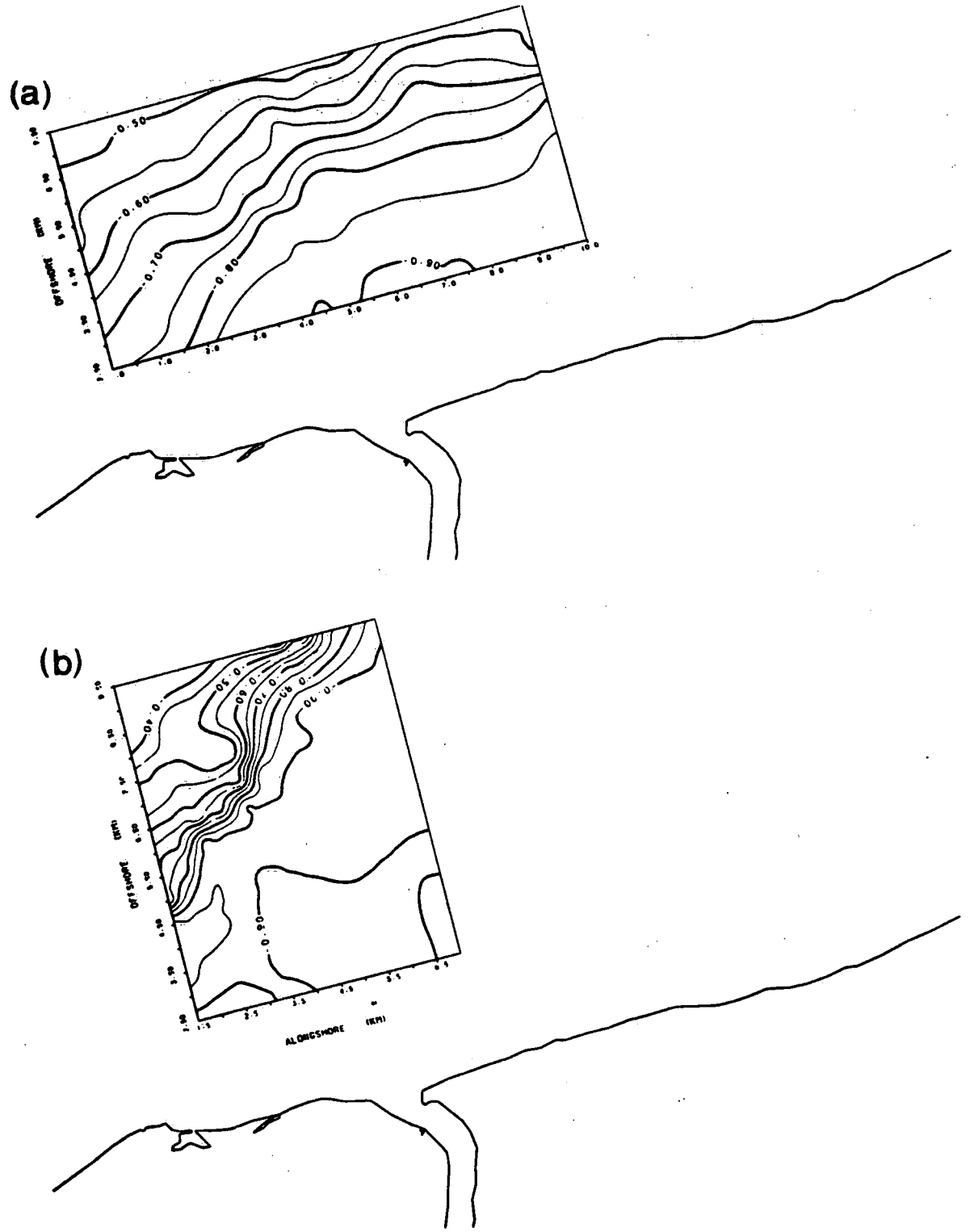
(a)
0.50
0.60
0.70
0.80
0.90
OFFSHORE (KM)
(b)
0.40
0.50
0.60
0.70
0.80
0.90
OFFSHORE (KM)
ALONGSHORE (KM)

Figure 3.7

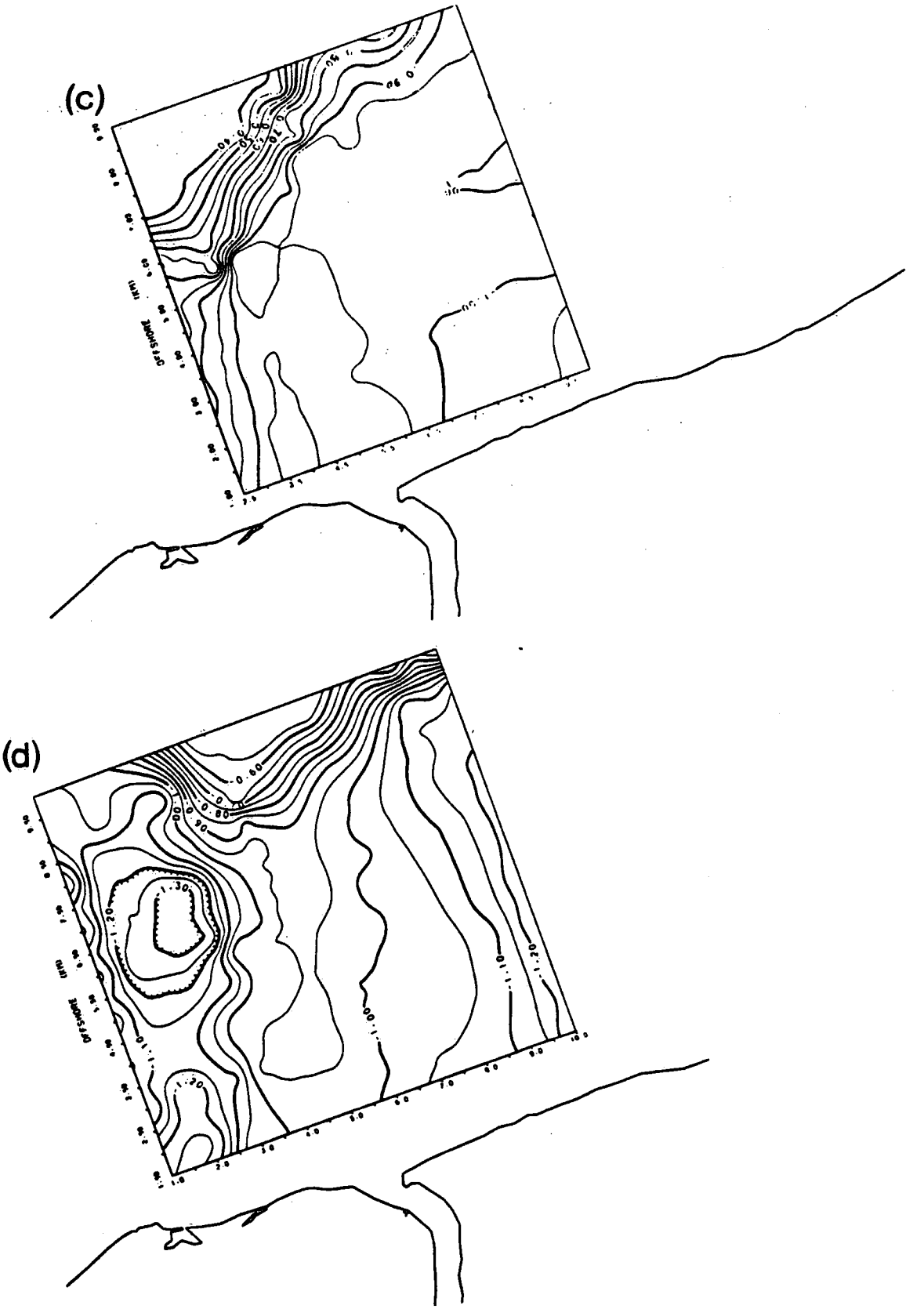

Figure 3.7

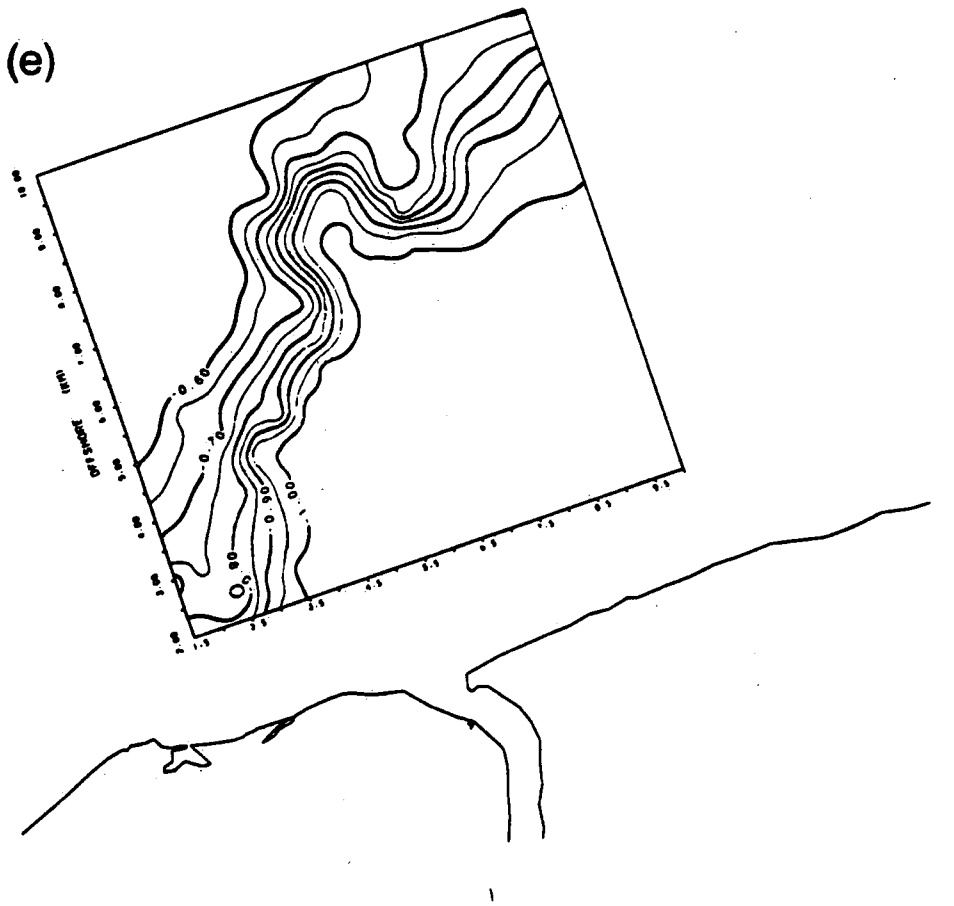

Figure 3.7

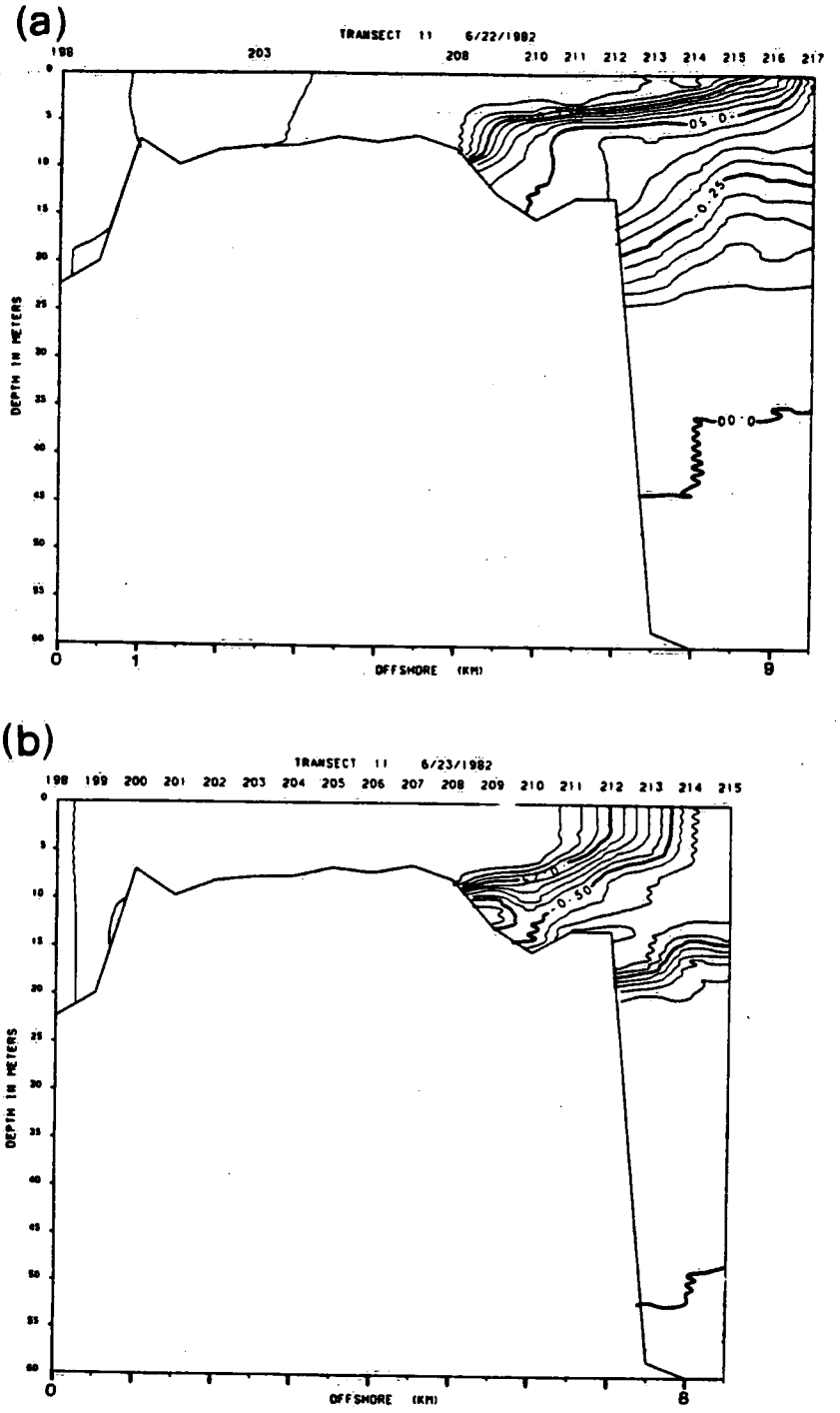
(a)
TRANSECT 11 6/22/1982
198 203 208 210 211 212 213 214 215 216 217
0.5
0.25
0.0
DEPTH IN METERS
0 1 OFFSHORE (KM) 9
(b)
TRANSECT 11 6/23/1982
198 199 200 201 202 203 204 205 206 207 208 209 210 211 212 213 214 215
1.0
0.50
DEPTH IN METERS
0 OFFSHORE (KM) 8

Figure 3.8

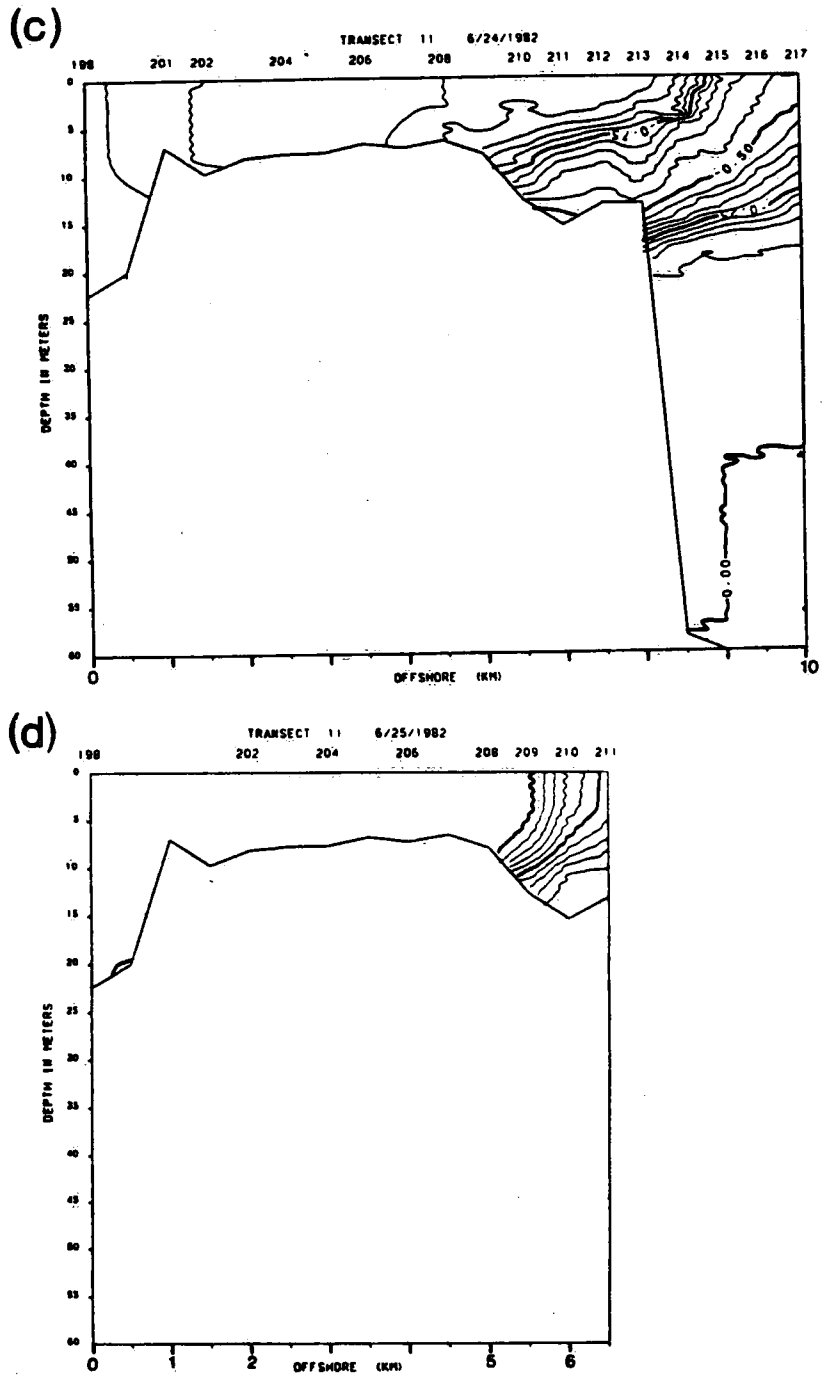
(c)
TRANSECT 11 6/24/1982
198 201 202 204 206 208 210 211 212 213 214 215 216 217
DEPTH IN METERS
0.50
0.00
0
OFFSHORE (KM)
10
(d)
TRANSECT 11 6/25/1982
198 202 204 206 208 209 210 211
DEPTH IN METERS
0 1 2 5 6
OFFSHORE (KM)

Figure 3.8

(a)

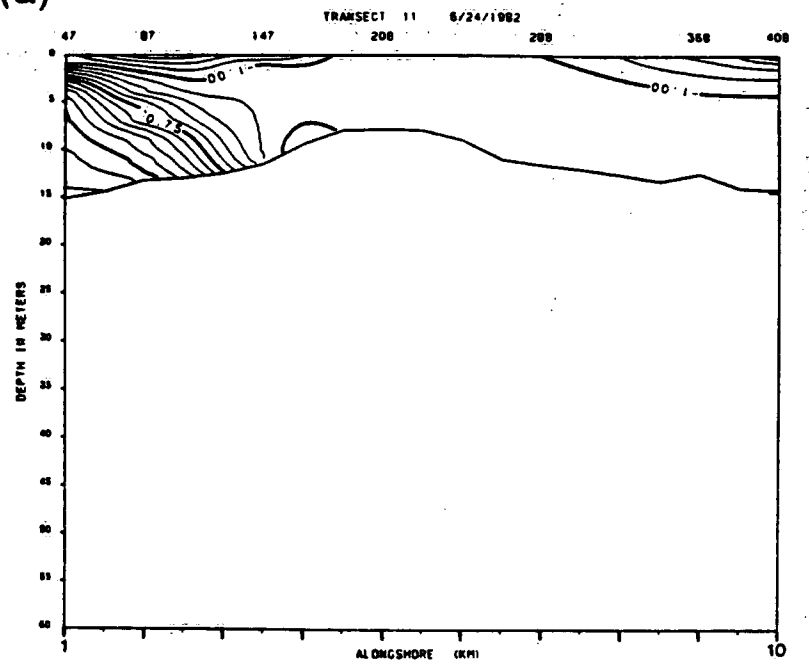
TRANSECT 11 6/24/1982
47 87 147 208 288 368 408
0.1
0.1
0.75
DEPTH IN METERS
ALONGSHORE (KM)
1
10

(b)

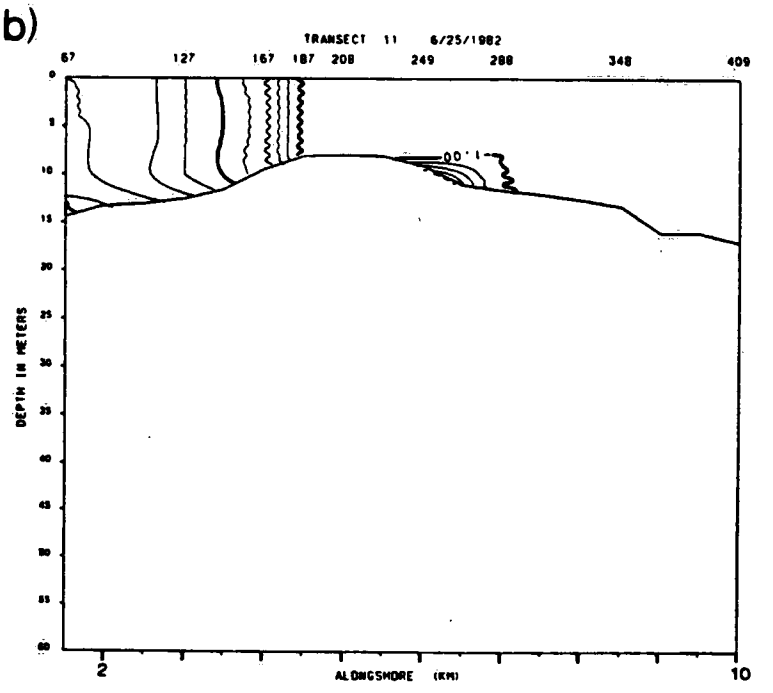
TRANSECT 11 6/25/1982
67 127 167 187 208 249 288 348 409
0.1
DEPTH IN METERS
ALONGSHORE (KM)
2
10

Figure 3.9

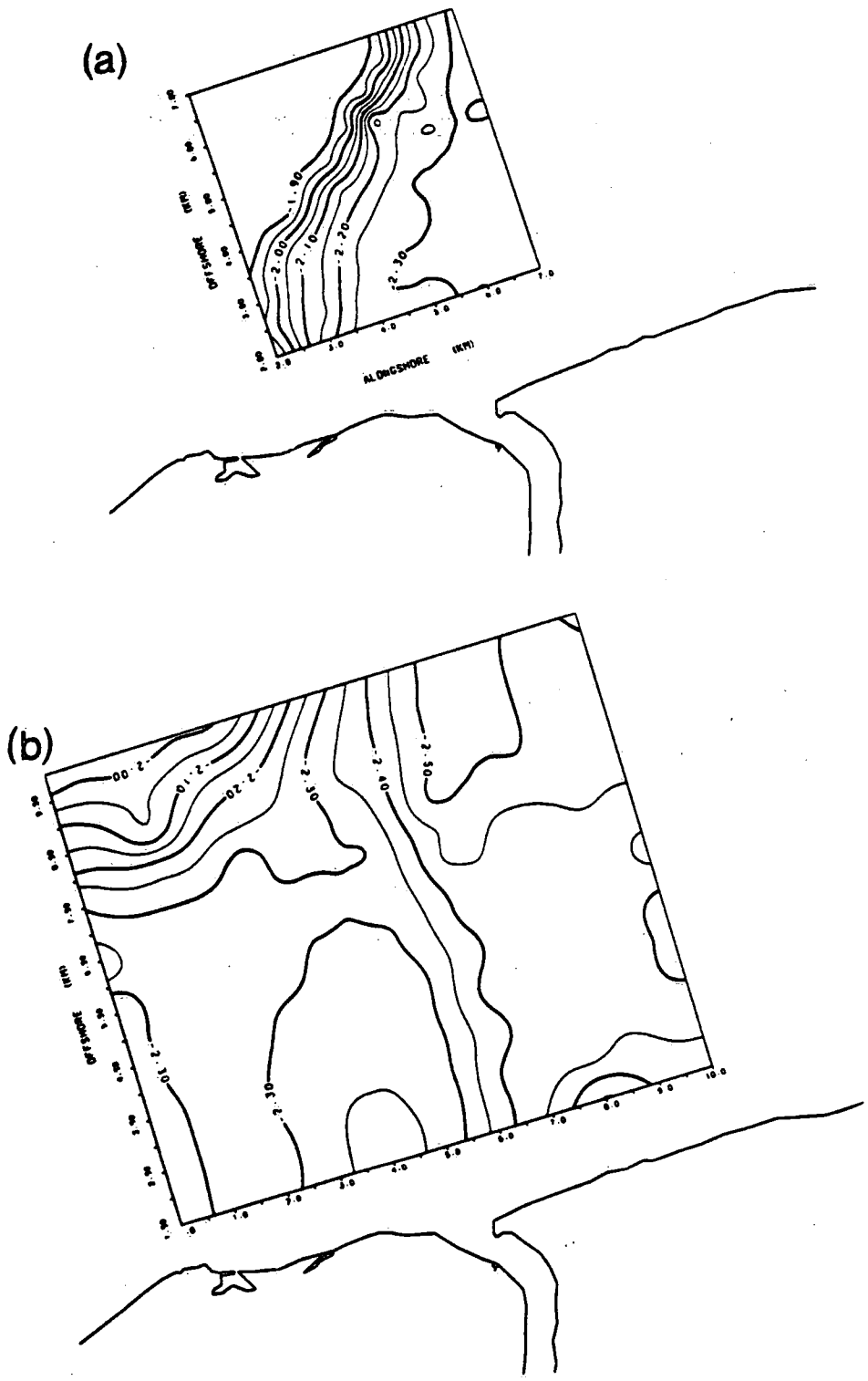
(a)
-2.00
-2.10
-2.20
-2.30
0
ALONGSHORE (KM)
(b)
-2.00
-2.10
-2.20
-2.30
-2.40
-2.50
-2.10
-2.30
ALONGSHORE (KM)

Figure 3.10

(a)

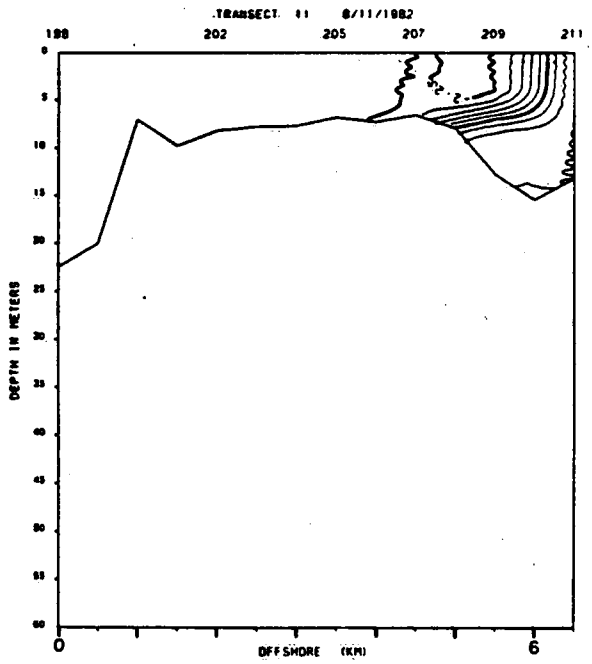

(b)

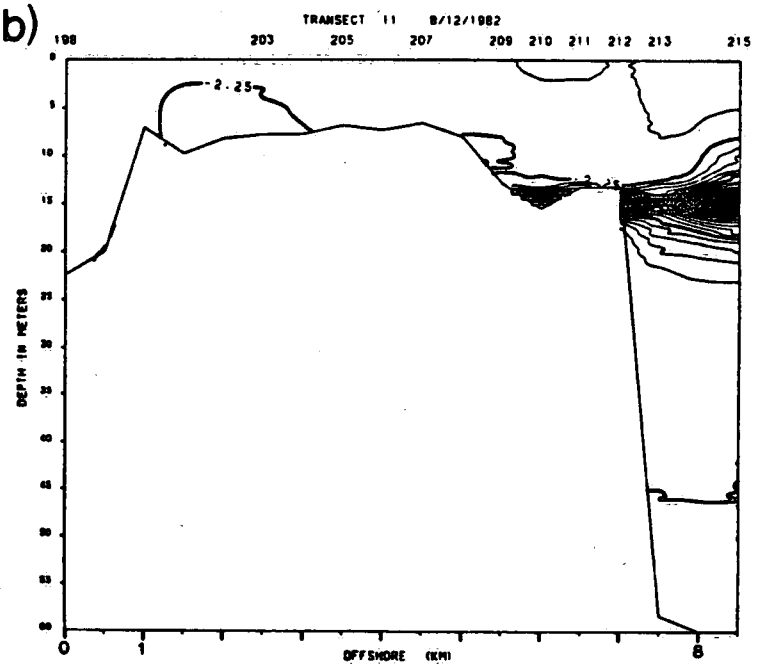

Figure 3.11

(a)

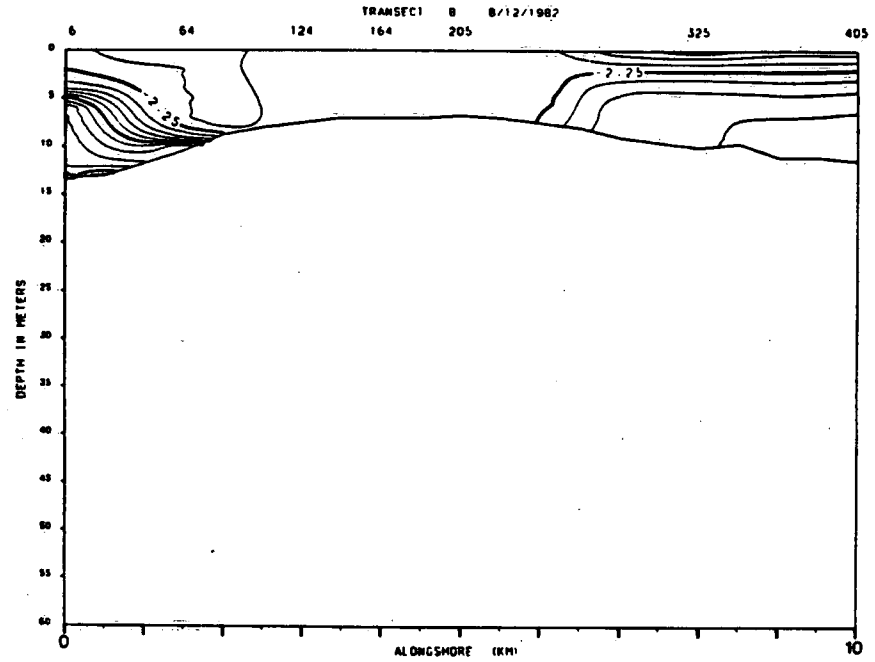

(b)

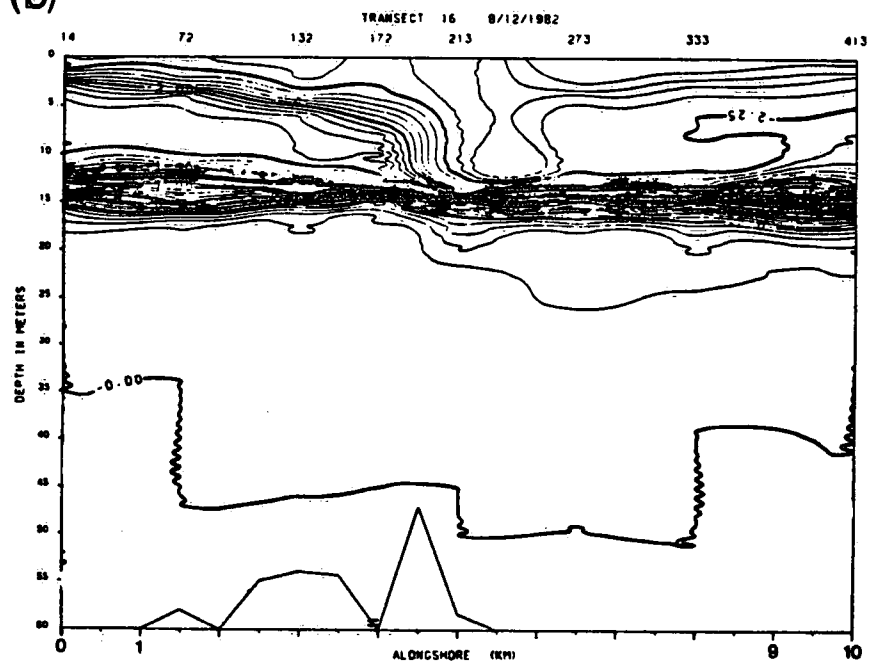

Figure 3.12

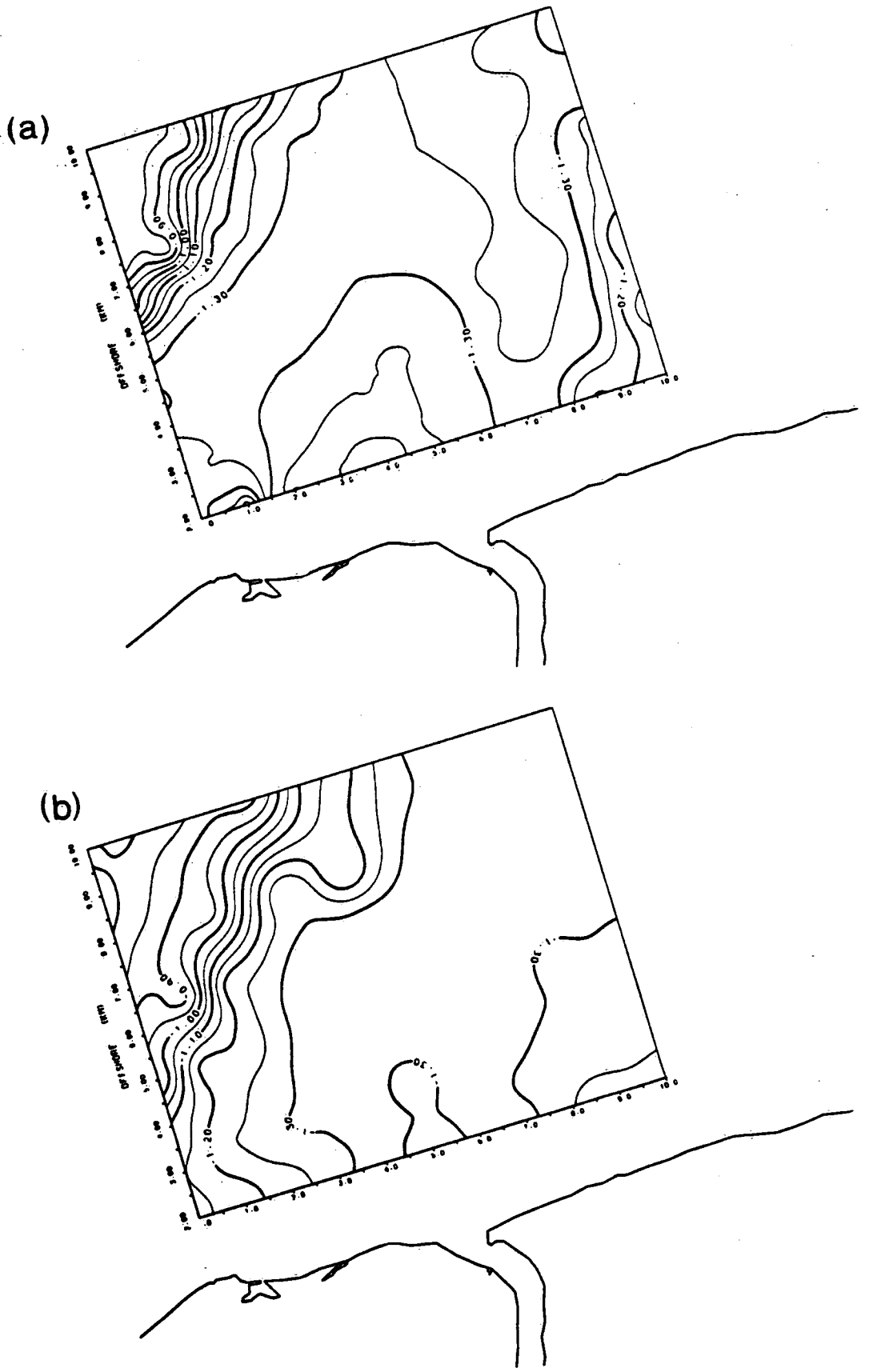

Figure 3.13

Figure 3.13

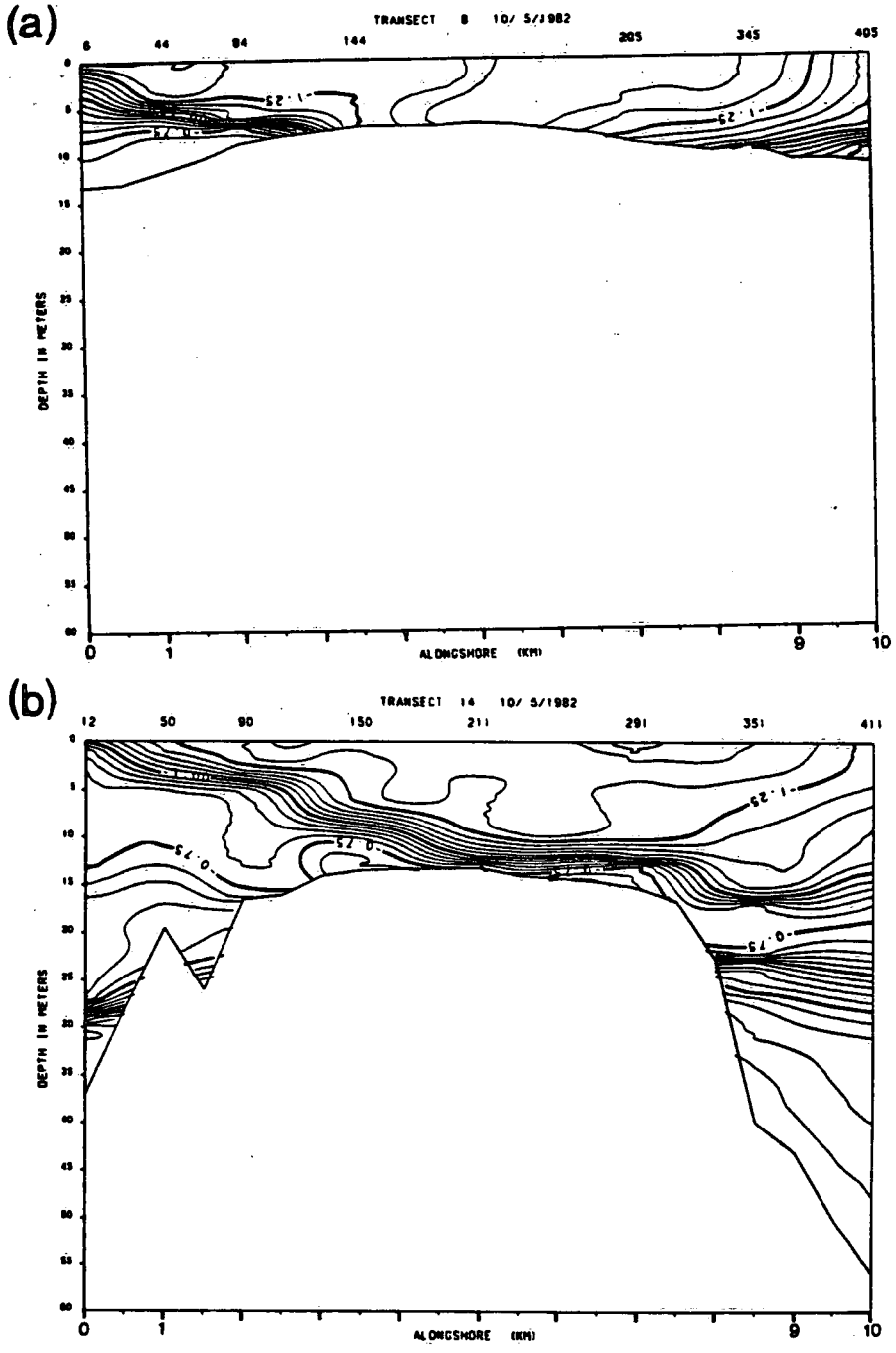
(a)
TRANSECT 8 10/ 5/1982
DEPTH IN METERS
ALONGSHORE (KM)
(b)
TRANSECT 14 10/ 5/1982
DEPTH IN METERS
ALONGSHORE (KM)

Figure 3.14

(c)

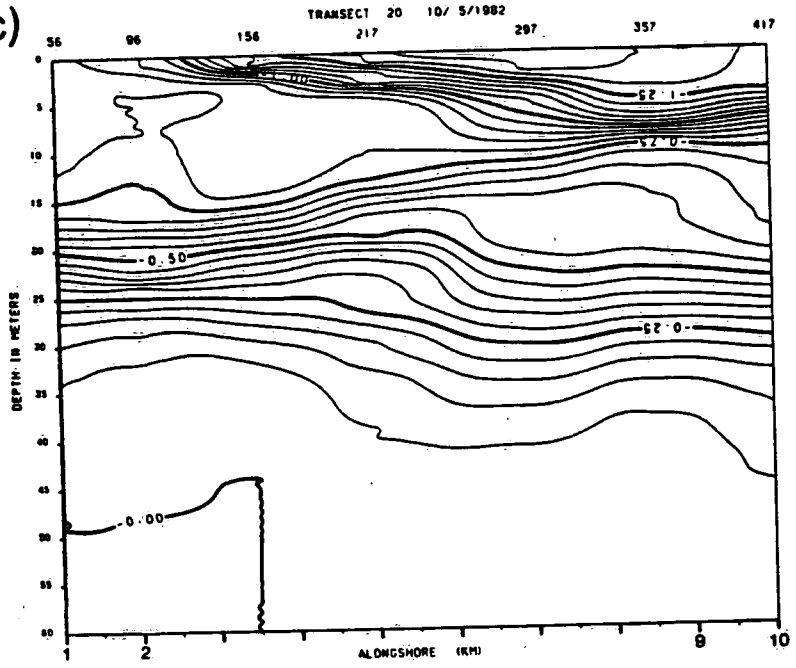
TRANSECT 20 10/ 5/1982
56
96
156
217
297
357
417
-1.25
-0.75
-0.50
-0.25
-0.00
DEPTH IN METERS
0
5
10
15
20
25
30
35
40
45
50
55
60
1
2
9
10
ALONGSHORE (KM)

Figure 3.14

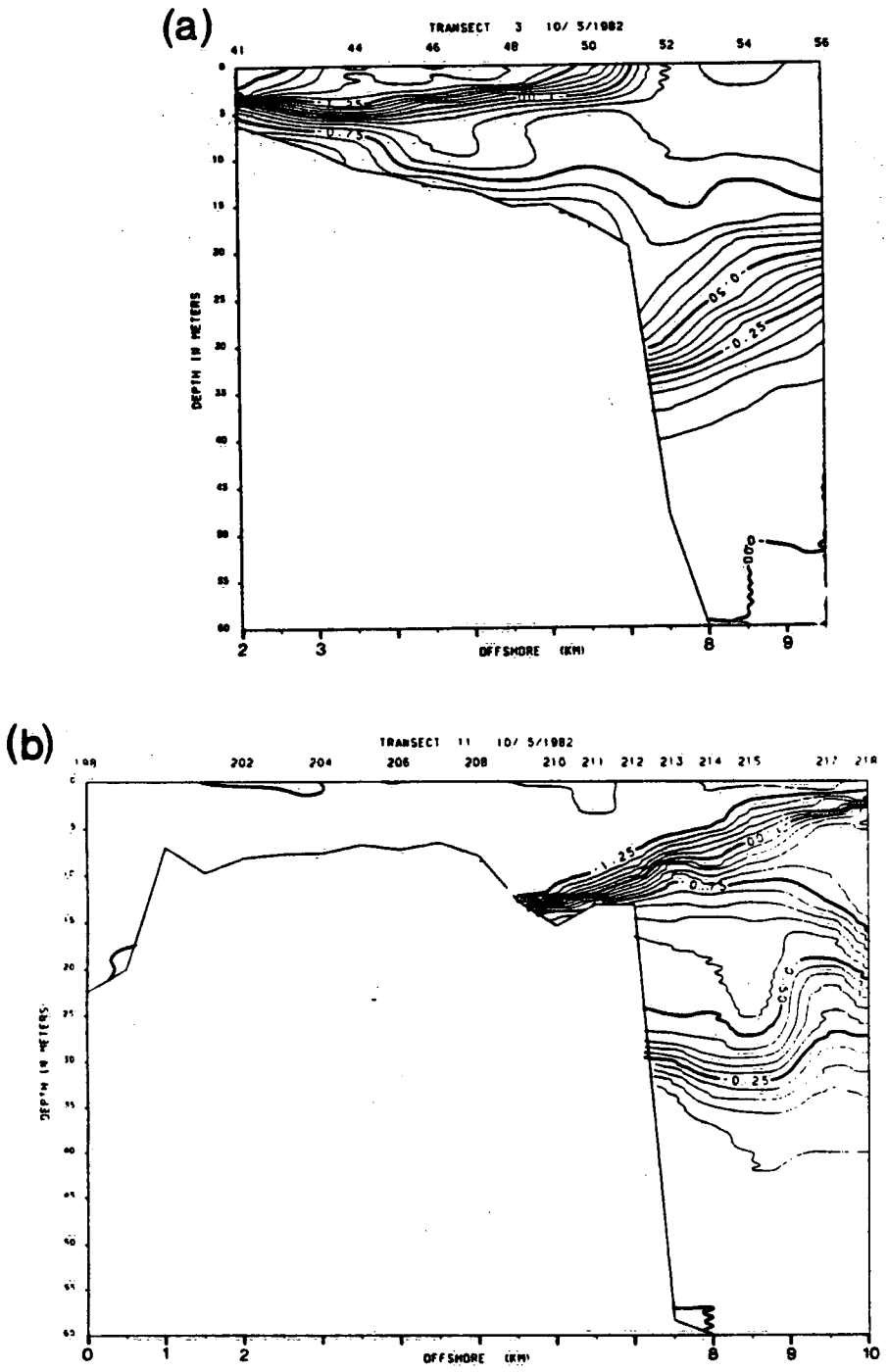
(a)
TRANSECT 3 10/ 5/1982
41 44 46 48 50 52 54 56
DEPTH IN METERS
OFFSHORE (KM)
2 3 8 9
(b)
TRANSECT 11 10/ 5/1982
202 204 206 208 210 211 212 213 214 215 217
DEPTH IN METERS
OFFSHORE (KM)
0 1 2 8 9 10

Figure 3.15

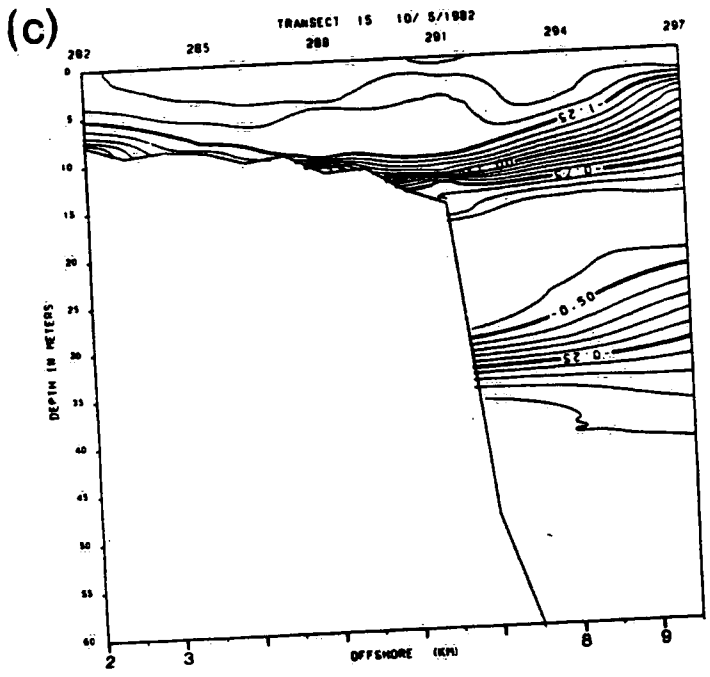
(c)
TRANSECT 15 10/ 5/1982
282
285
288
291
294
297
DEPTH IN METERS
-1.25
-0.75
-0.50
-0.25
2
3
OFFSHORE (KM)
8
9

Figure 3.15

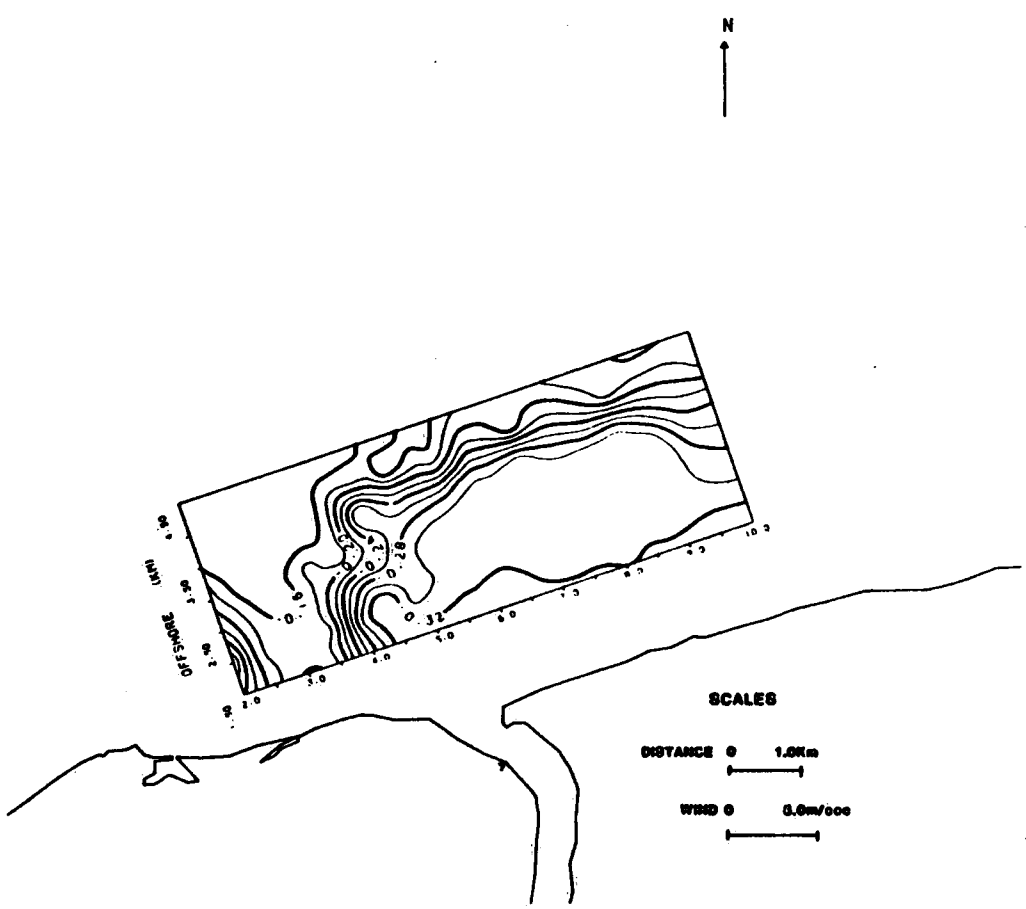
N
OFFSHORE (km)
SCALES
DISTANCE 0 1.0Km
WIND 0 5.0m/sec

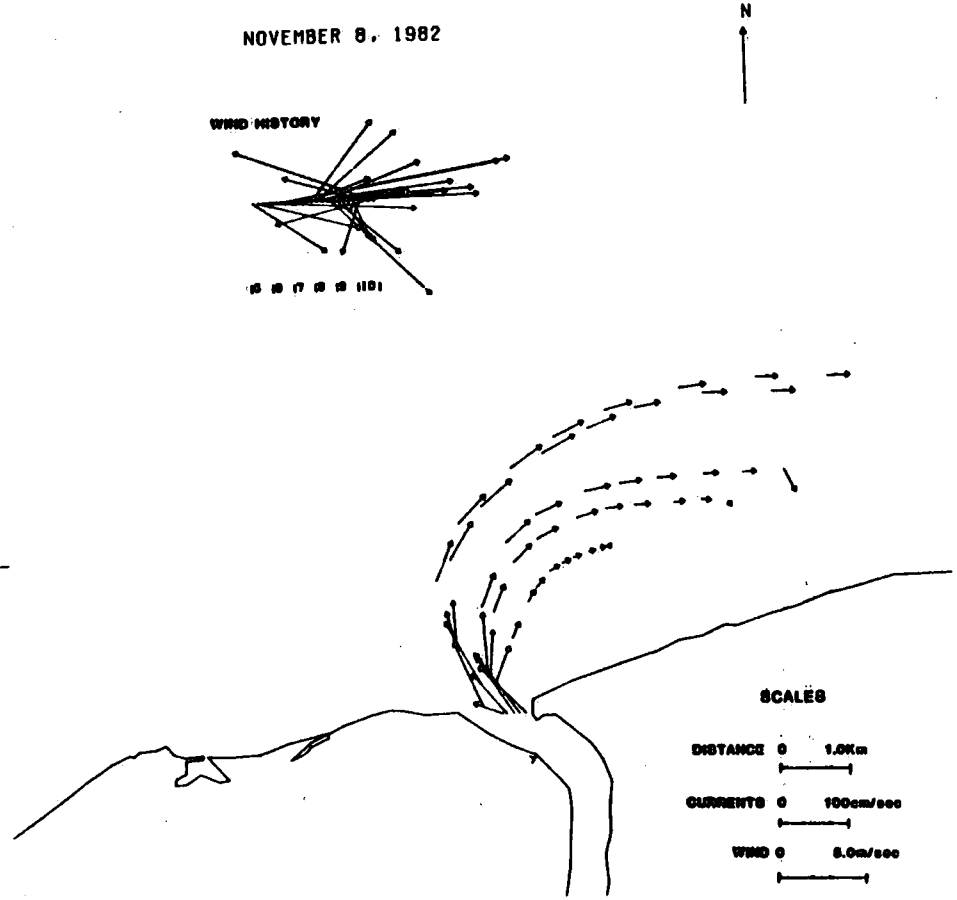
NOVEMBER 8, 1982
N
WIND HISTORY
SCALES
DISTANCE 0 1.0Km
CURRENTS 0 100cm/sec
WIND 0 5.0m/sec

Figure 3.16

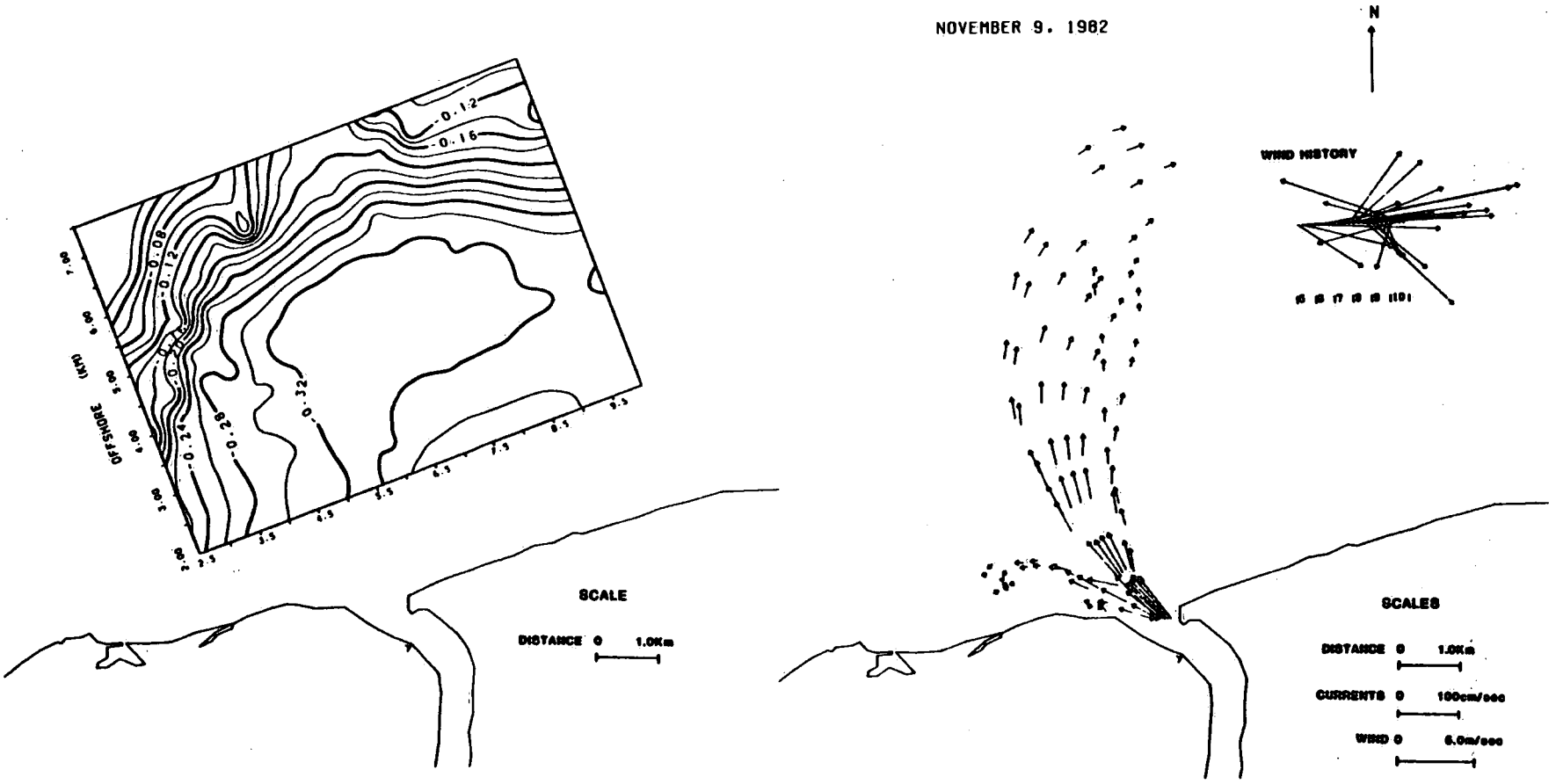
NOVEMBER 9. 1982
N
WIND HISTORY
OFFSHORE (KM)
SCALE
DISTANCE 0 1.0Km
SCALES
DISTANCE 0 1.0Km
CURRENTS 0 100cm/sec
WIND 0 5.0m/sec

Figure 3.17

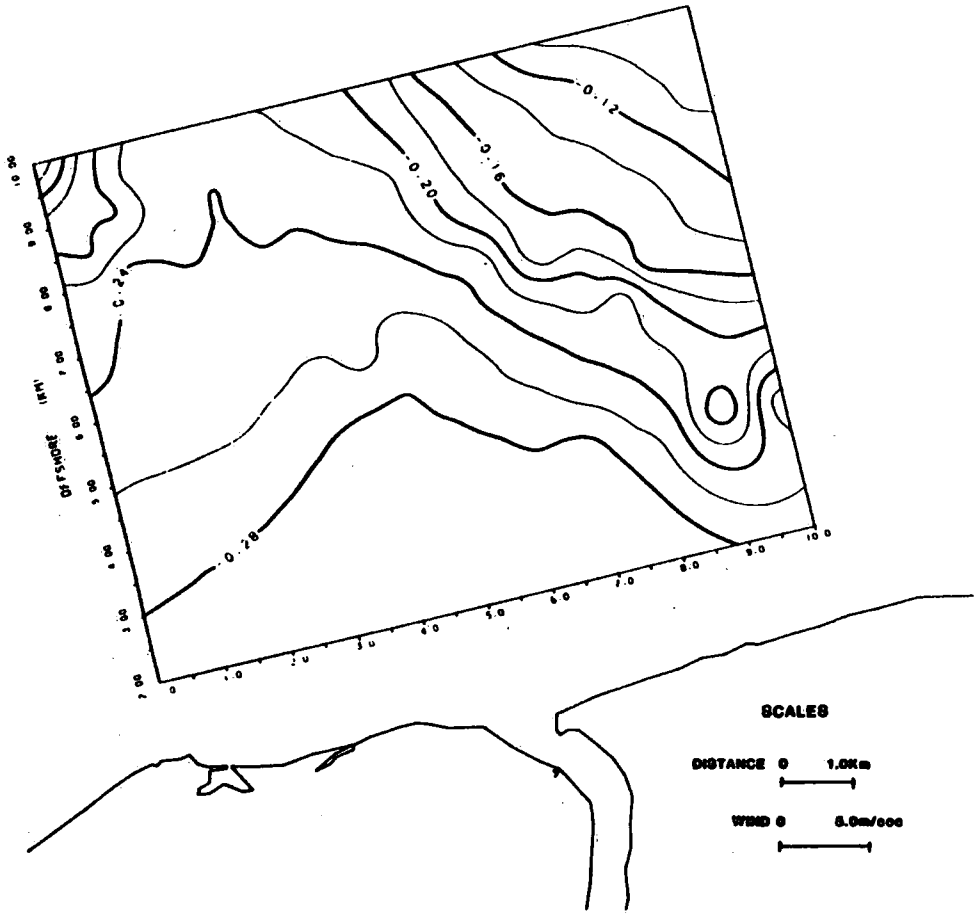
-0.12
-0.16
-0.20
-0.24
-0.28
OFFSHORE (KM)
SCALES
DISTANCE 0 1.0Km
WIND 0 5.0m/sec

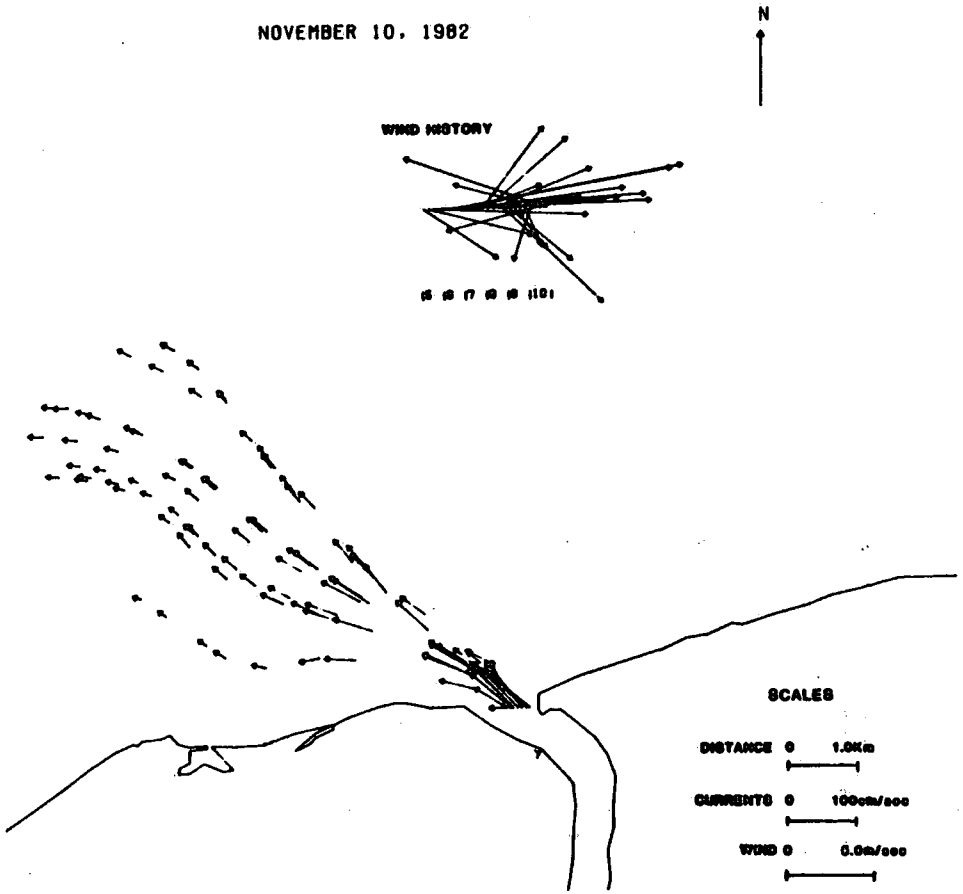
NOVEMBER 10, 1982
N
WIND HISTORY
SCALES
DISTANCE 0 1.0Km
CURRENTS 0 100cm/sec
WIND 0 5.0m/sec

Figure 3.18

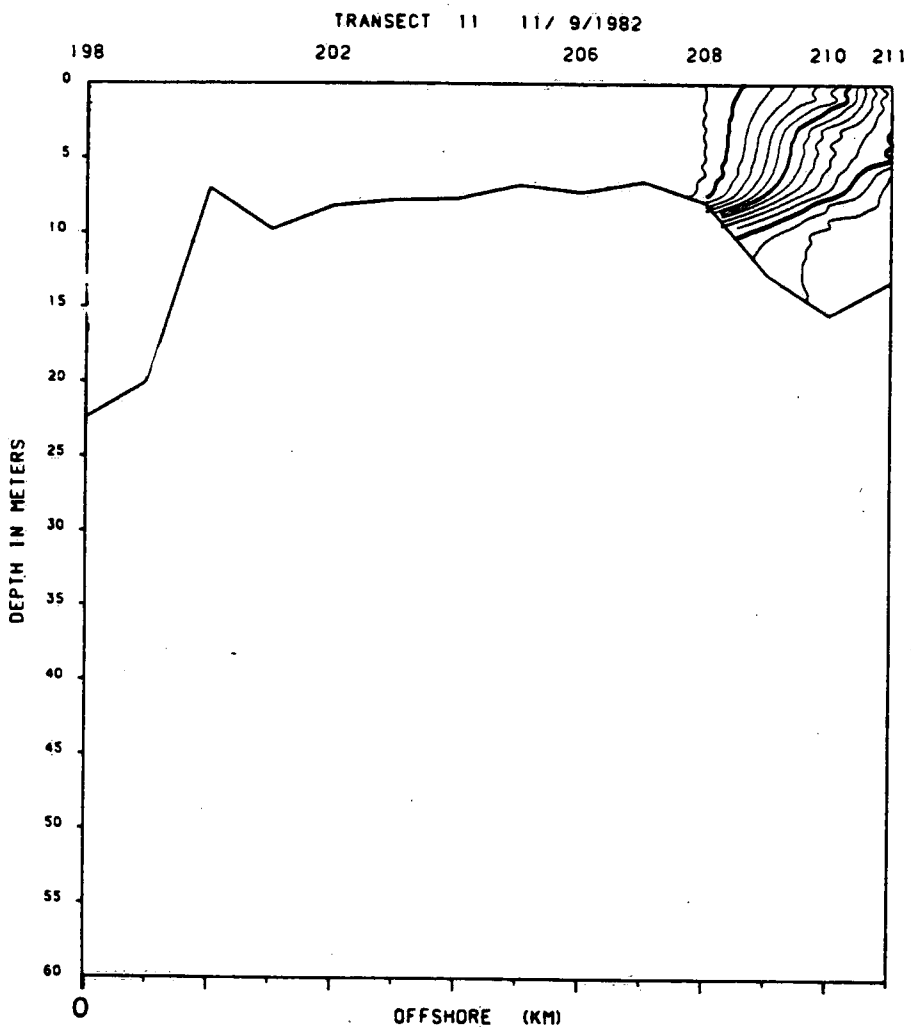
TRANSECT 11 11/ 9/1982
198
202
206
208
210
211
0
5
10
15
20
25
30
35
40
45
50
55
60
DEPTH IN METERS
0
OFFSHORE (KM)

Figure 3.19

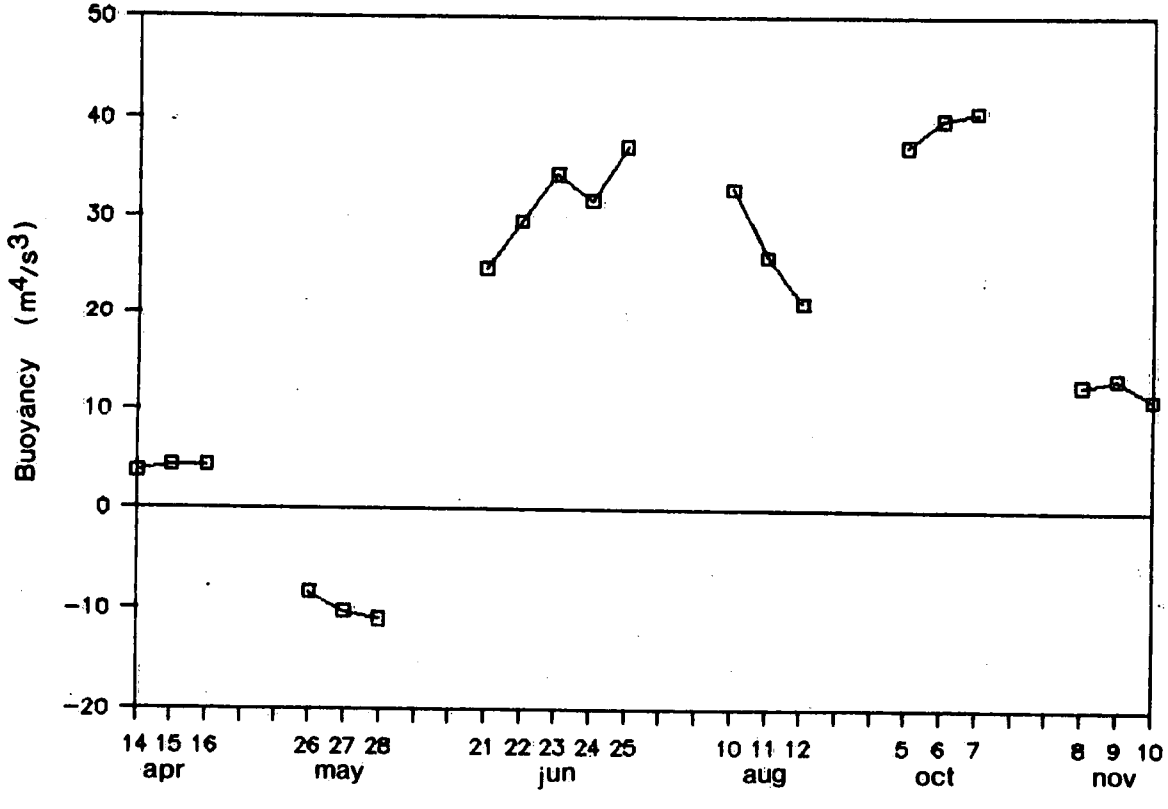
Buoyancy (m4/s3)
50
40
30
20
10
0
-10
-20
14 15 16
apr
26 27 28
may
21 22 23 24 25
jun
10 11 12
aug
5 6 7
oct
8 9 10
nov

Figure 4.1

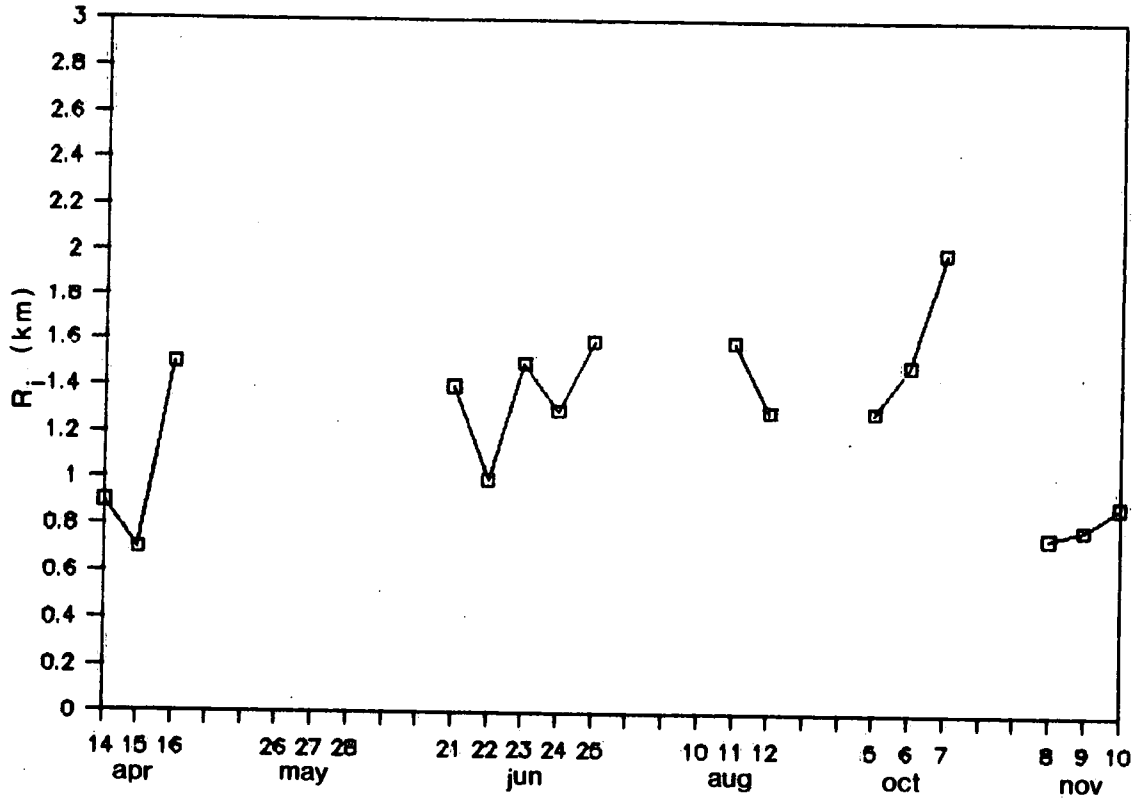
3
2.8
2.6
2.4
2.2
2
1.8
1.6
1.4
1.2
1
0.8
0.6
0.4
0.2
0
R_i (km)
14 15 16
apr
26 27 28
may
21 22 23 24 25
jun
10 11 12
aug
5 6 7
oct
8 9 10
nov

Figure 4.2

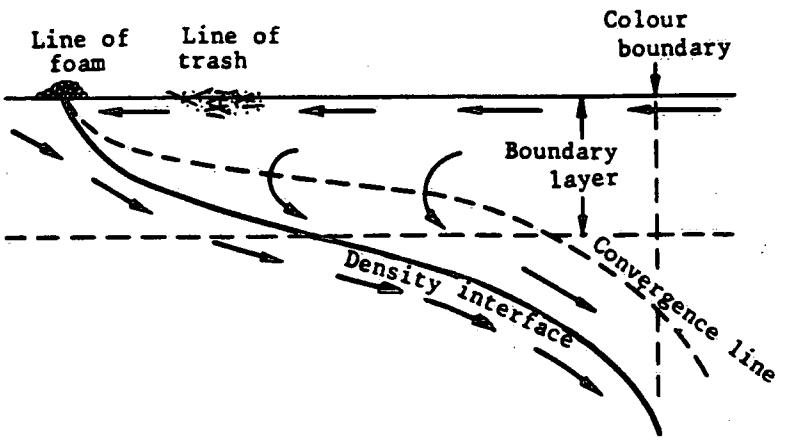

Figure 4.3

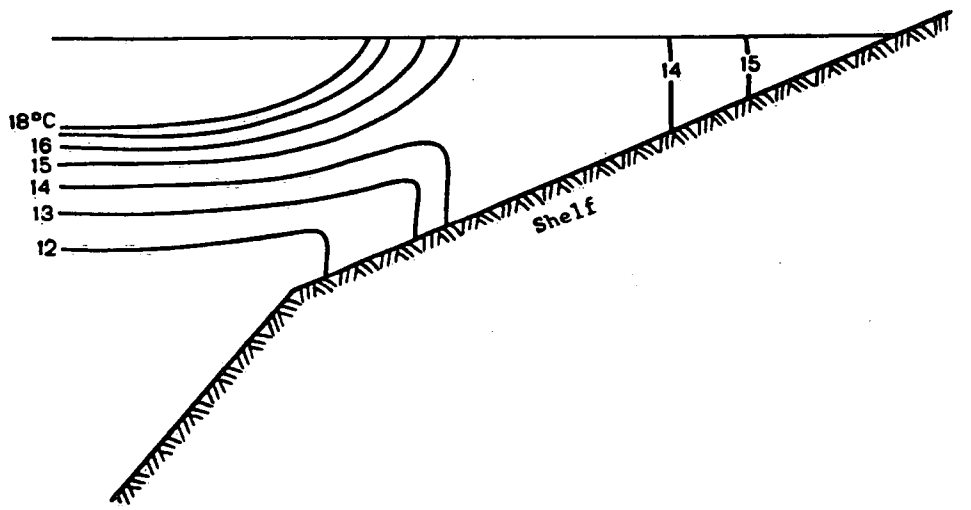

Figure 4.4

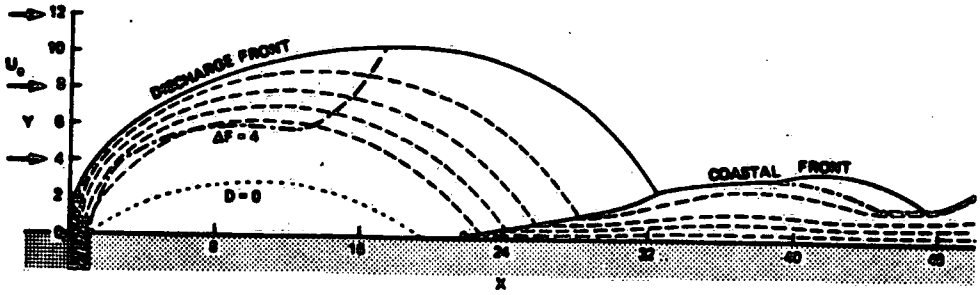
12
10
8
6
4
2
0
U_0
V
DISCHARGE FRONT
ΔF = 4
D = 0
COASTAL FRONT
8
16
24
32
40
48
X

Figure 4.5